# Methods of Measuring the Properties of Ionized Gases at Microwave Frequencies

SANBORN C. BROWN
MANFRED A. BIONDI
MELVIN A. HERLIN
EDGAR EVERHART
DONALD E. KERR

TECHNICAL REPORT NO. 66

MAY 17, 1948

RESEARCH LABORATORY OF ELECTRONICS

MASSACHUSETTS INSTITUTE OF TECHNOLOGY

The research reported in this document was made possible through support extended the Massachusetts Institute of Technology, Research Laboratory of Electronics, jointly by the Army Signal Corps, the Navy Department (Office of Naval Research), and the Air Force (Air Materiel Command), under the Signal Corps Contract No. W-36-039 sc-32037.

MASSACHUSETTS INSTITUTE OF TECHNOLOGY
Research Laboratory of Electronics

Technical Report No. 66 May 17, 1948

# METHODS OF MEASURING THE PROPERTIES OF IONIZED GASES AT MICROWAVE FREQUENCIES

Sanborn C. Brown
Manfred A. Biondi
Edgar Everhart
Melvin A. Herlin
Donald E. Kerr

## Abstract

Microwave measurement techniques, devised especially for microwave gas-discharge measurements but applicable generally, are discussed here. Measurement of cavity Q's from standing-wave patterns, including the effect of series loss in the input lead, is described. In addition to the standard half-power-point method, a method is given for obtaining the external Q from the slope of the curve of the position of the voltage minimum vs. wavelength. Methods of determining the electric field from measurements of power and cavity parameters are discussed, and these methods are extended to low-Q cases, encountered with heavy discharge currents, by means of a four-terminal network theory. The complex conductivity (or the equivalent complex dielectric coefficient) is discussed from the cavity and four-terminal network points of view for low and high discharge current densities, respectively. Measurements of transient discharge phenomena are treated through the transient resonant frequency measurement in transmission and reflection, and through the transient measurements of the standing-wave pattern.

## Contents

## Introduction

This report has been written primarily to introduce workers in the field of gas discharges to the techniques used in measuring the properties of ionized gases at microwave frequencies. Since, however, several new microwave techniques have been devised, it should also be of interest to the general microwave experimenter.

The phenomena associated with gas discharges at microwave frequencies are in general much simpler than those corresponding to d-c discharges. On the other hand, the microwave techniques are not so well known and may therefore discourage workers from entering the field. Experience in this laboratory has shown that the readily available texts on ultra-high frequency measurements do not include the particular calculations of the Q, the electric field, or the conductivity in the most convenient or workable form for gas-discharge measurements. To fill this need the present report was prepared. The report does not start at an elementary level but assumes familiarity with the basic concepts and techniques of the microwave field.

In the study of ionization processes, breakdown, and low current-density discharge phenomena, high-Q devices can be used. For high current-density discharges, low-Q devices have to be used. Thus, methods for determining physical quantities, such as field strength and complex conductivity, are discussed in both high- and low-Q devices.

In the problem of calculating the Q of resonant cavities used in the gas-discharge measurements, the necessary accuracy is not achieved if one neglects the series losses between the cavity and the reference plane to which the measurements are referred. Also since the width of the Q curves are determined by the total loading of the cavity, the loaded Q gives the best coverage of the parameters. For these reasons a method of determining the Q with a series loss included, in terms of the loaded Q, has been worked out. This extends the Q determinations of Lawson in which the calculations were made neglecting the series loss, and differs from the method developed by Slater which included the series loss but was calculated in terms of the external Q. When the Q's of the cavities are very low, accurate determinations of the parameters are best obtained by calculating the Q from the slope of the phase curve; therefore this method is also described.

One of the important parameters which controls the physical behavior of the gas discharge is the value of the electric field in which the electrons are accelerated. The ease with which the electric field configuration in a resonant cavity can be calculated depends to a large extent on the cavity design. Since the requirements of the gas discharge are not necessarily consistent with simple field configuration requirements, three ways of determining the field in a cavity have been developed.

The simplest method for calculating the electric field applies to those cases in which the mode of oscillation is sufficiently well known to allow a quantity like the capacitance to be calculated. The ordinary capacitance can be defined as the ratio of the stored energy to the square of the voltage whereas for the present considerations it is more convenient to define a new quantity which is similar to capacitance but is defined as the ratio of the stored energy to the square of the field.

For cavities having complicated shapes a method of calculating the electric field is described which is determined by measuring the shift in the cavity resonant frequency by inserting a small metal plug into the high-field region. For cases in which the Q of the cavity is so low that simple cavity theory does not apply, a network theory method of determining the electric field is also derived.

In the study of gas discharges, in addition to the electric field, the complex conductivity of the discharge is an important parameter. To obtain this, one measures standing-wave ratio and phase in the input line and converts these into values of conductance and susceptance of the discharge. The determinations of these quantities are outlined. Cavity theory is conveniently used for discharges which are studied in cavity resonators whose normalized admittances are greater than 100. On the other hand when the normalized admittance is low, of the order of 20, complications introduced by the other modes in the cavity require the use of a four-terminal network method.

Special problems arise when transient discharge phenomena are measured. Three different techniques for these measurements are discussed. Two of these involve the resonant frequency shift of a high-Q cavity, one a transmission method and the other a reflection method. The third method of studying transient phenomena involves an electronic method of measuring transient standing-wave patterns.

## Section 1. Q MEASUREMENTS

1.1. Q with Series Loss. Two of the important parameters of a cavity to be measured are the Q and the wavelength. The Q is defined by the relation:

$$Q = \frac{\text{energy stored}}{\text{energy dissipated per radian}} . \qquad (1\text{-}1)$$

Various kinds of Q's may be discussed depending on where it is convenient, in a particular problem, to consider the energy to be dissipated. In experiments for determining the electric field intensity in a resonant cavity from measurements of input power and the standing-wave pattern in the input line, one is led to the following considerations. It is justifiable to represent the problem of a resonant cavity in a line which includes a series loss, by the equivalent circuit of Fig. 1-1(a). In this equivalent circuit, the series

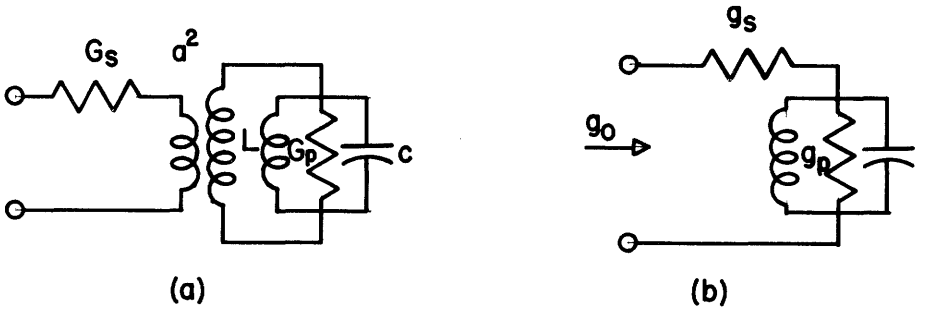


Fig. 1-1. Equivalent circuits for a resonant cavity.

loss represented by the conductance $G_s$ includes losses in the cavity coupling loop, glass seals, and polystyrene insulators, up to the reference plane from which the voltage standing-wave minima are measured. The normalized admittance of the cavity may be written as:

$$y_c = \frac{a^2}{Y_o}\sqrt{\frac{C}{L}} \qquad (1\text{-}2)$$

where $a^2$ is the admittance transformer ratio, $Y_o$ the characteristic admittance of the input line, C and L the capacitance and inductance of the cavity, respectively. The equivalent circuit for the normalized quantities is shown in Fig. 1-1(b).

With the cavity on resonance, the reactance of the capacitance and inductance disappears and the conductance looking into the circuit is $g_o$. Then from Ohm's law

$$g_p = \frac{g_o}{1-\left(\frac{g_o}{g_s}\right)} . \qquad (1\text{-}3)$$

The experimental determination of a Q curve consists in measuring the standing-wave ratio in the input line as a function of the wavelength $\lambda$. The phase curves are determined by plotting the position of minimum of the standing wave as a function of the wavelength. One may define a loaded Q, which is a measure of the width of the Q curve determined experimentally, by considering the cavity to be internally excited and writing down expressions for the energy stored divided by the energy dissipated per radian looking from the cavity, back toward the line. This will lead to a defining equation for the loaded Q of the form

$$Q_L = \frac{y_c}{g_p + \frac{g_s}{1 + g_s}} . \qquad (1\text{-}4)$$

To be able to calculate the value for $Q_L$ we must derive an expression to determine the half-power points on the Q curve. The condition which must be satisfield at the half-power points is

$$b_r = (g_p + \frac{g_s}{1 + g_s}) \qquad (1\text{-}5)$$

where $b_r$ is the normalized susceptance of the cavity. Under these conditions, the normalized admittance at the half-power points is

$$y_r = g_p + j(g_p + \frac{g_s}{1 + g_s}), \qquad (1\text{-}6)$$

and the impedance is

$$z_r = \frac{1}{y_r} = r_r + jx_r. \qquad (1\text{-}7)$$

Adding in the effect of the series conductance, we have

$$z = \frac{1}{g_s} + r_r + jx_r = r + jx. \qquad (1\text{-}8)$$

The reflection coefficient, which is defined as the complex ratio of the reflected voltage to the incident voltage at the reference plane, will be

$$\Gamma = \frac{z - 1}{z + 1} = \frac{r + jx - 1}{r + jx + 1}$$

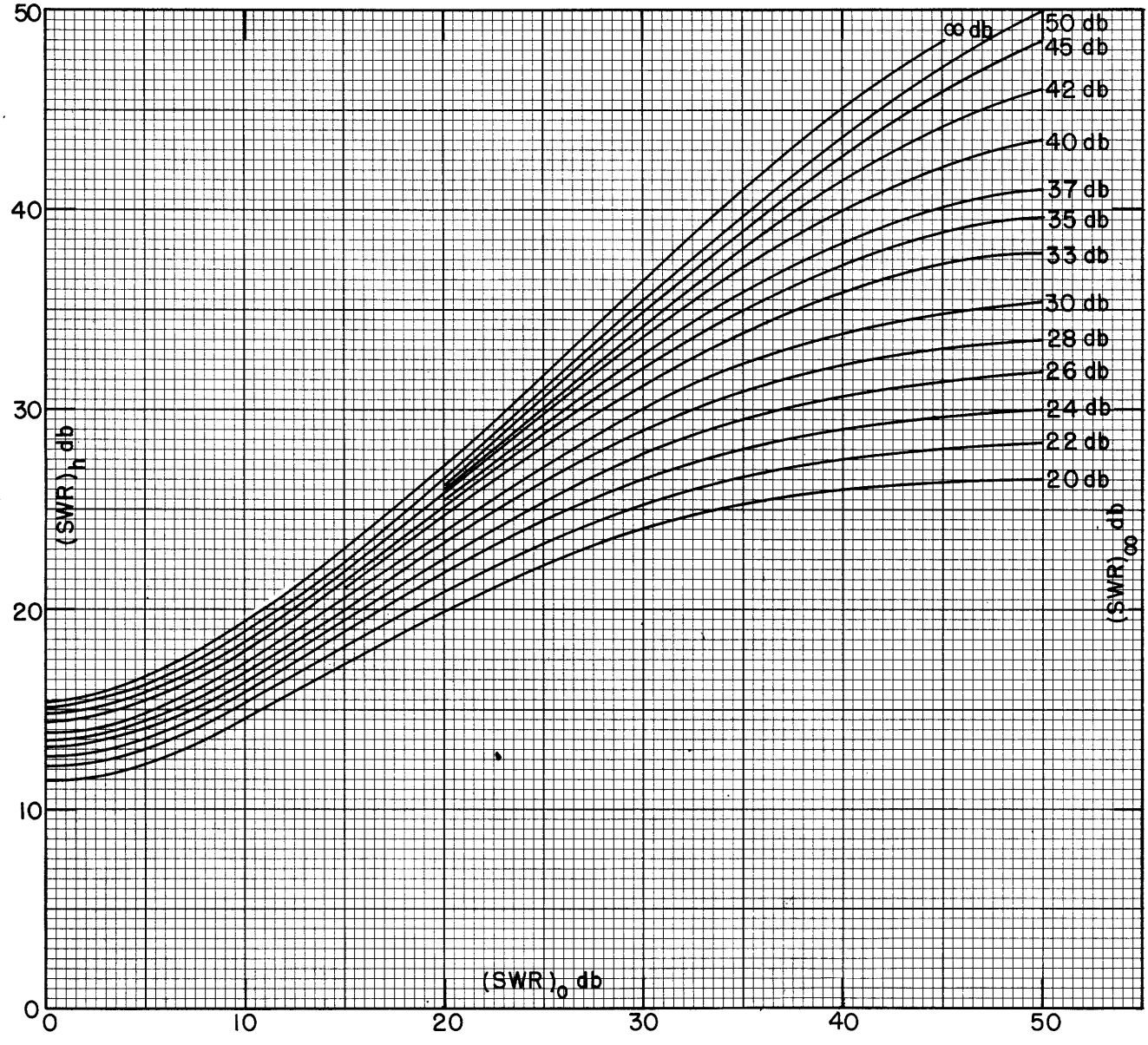


Fig. 1-2. Standing-wave ratio at the half-power points as a function of the standing-wave ratio on resonance.

$$|\Gamma| = \sqrt{\frac{(r-1)^2 + x^2}{(r+1)^2 + x^2}} .$$

In terms of the reflection coefficient, the voltage standing-wave ratio at the half-power points is given by the relations

$$(VSWR)_h = \frac{1 + |\Gamma|}{1 - |\Gamma|} = \frac{\sqrt{\left(\frac{r+1}{x}\right)^2 + 1} + \sqrt{\left(\frac{r-1}{x}\right)^2 + 1}}{\sqrt{\left(\frac{r+1}{x}\right)^2 + 1} - \sqrt{\left(\frac{r-1}{x}\right)^2 + 1}} \quad . \qquad (1\text{-}9)$$

From these expressions and the relation that

$$(SWR)_{db} = 20 \log_{10}(VSWR)$$

we may put these equations into the useful form of Fig. 1-2.

In Fig. 1-2, we have plotted the standing-wave ratio in db at the half-power points against the $(SWR)_{db}$ on resonance. The family of curves are plotted for different values of the series loss and are calculated in terms of the off-resonance $(SWR)_{\infty\, db}$ which would actually be observed in an experimental measurement of a Q curve. The values of $(SWR)_{o\ db}$, the db standing-wave ratio on resonance, are considered positive when $g_s$ is less than unity and negative if $g_s$ is greater than unity. The curves of Fig. 1-2 are symmetrical about the origin and hence can be used for either positive or negative values of $(SWR)_{o\ db}$.

Determination of the values of $Q_L$ may be done in the following manner. By plotting the value of $(SWR)_{db}$ against $\lambda$, a curve similar to that shown in Fig. 1-3 is obtained. With the values thus obtained for

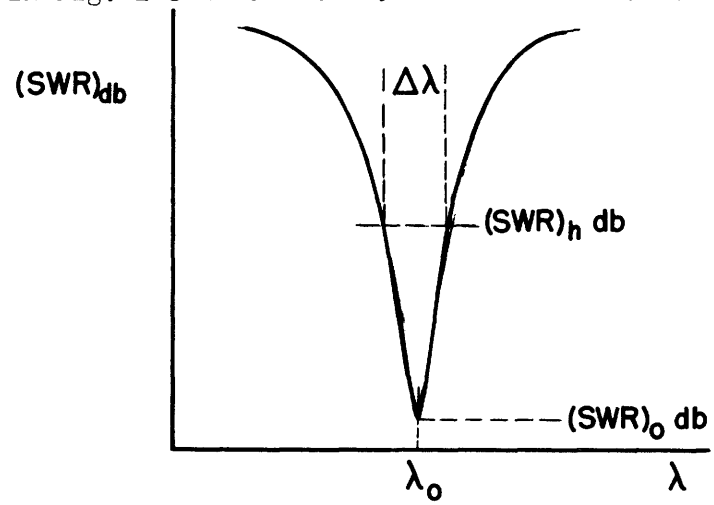


Fig. 1-3. Typical experimental Q curve.

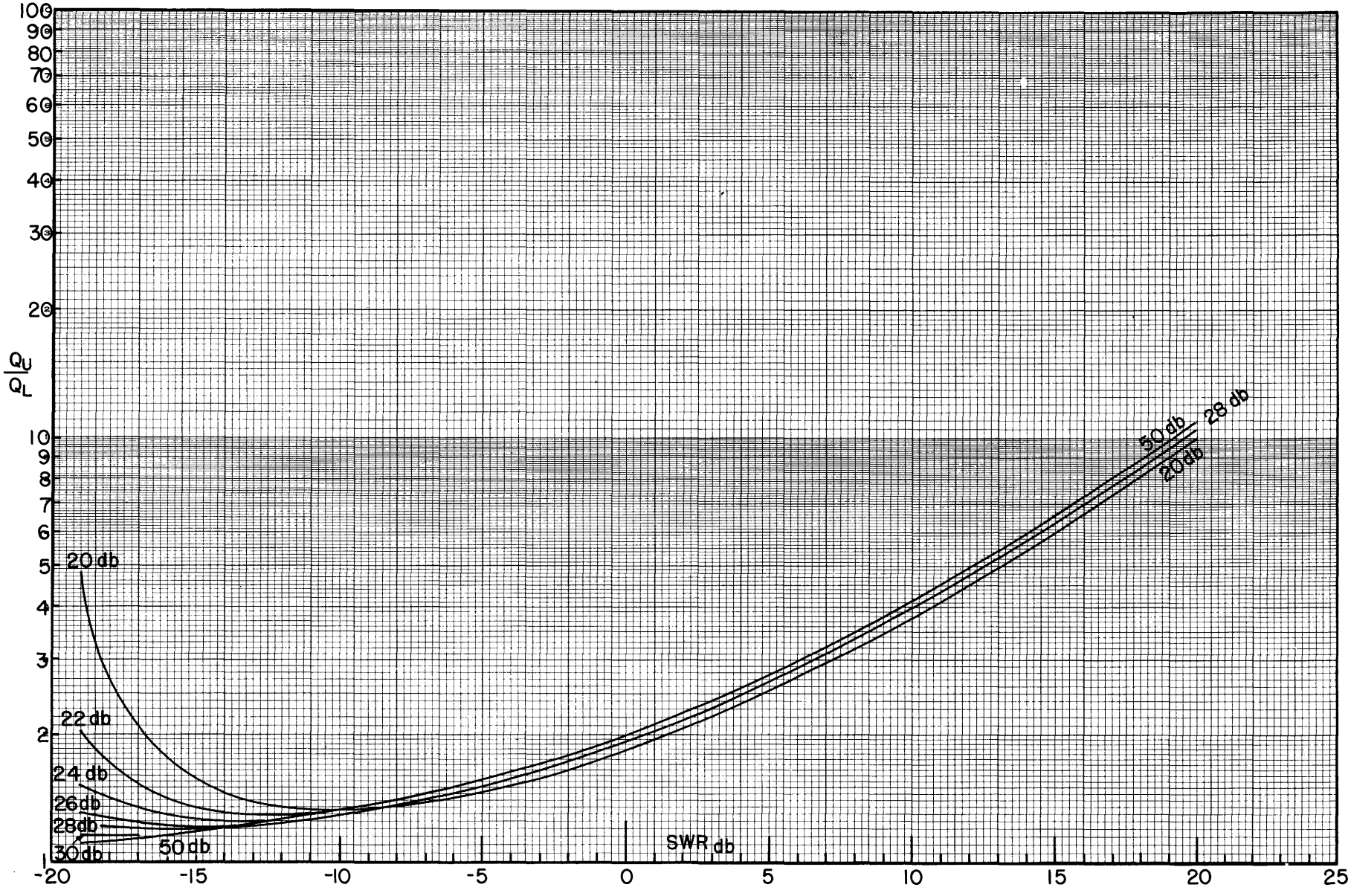


Fig. 1-4. The ratio of unloaded to loaded Q's plotted as a function of the standing-wave ratio on resonance.

$(SWR)_{\infty\,db}$ and $(SWR)_{o\ db}$ one enters the family of curves in Fig. 1-2 and reads from the ordinate a value for $(SWR)_{h\ db}$. Entering the Q-curve plot again, one may determine the width of the Q curve at this point, thereby defining a $\Delta\lambda$ such that

$$Q_L = \frac{\lambda_o}{\Delta\lambda} \cdot \tag{1-10}$$

We consider the cavity, which is to be excited externally, to be in series with the loss of $g_s$, and calculate the ratio of energy stored in the cavity to the energy dissipated in $g_s$ and $g_o$ per radian. This ratio defines the unloaded Q as used in this report. The equation for the unloaded Q is of the form:

$$Q_U = \frac{y_c}{g_o\left(1 + \frac{g_o}{g_s}\right)} \cdot \tag{1-11}$$

Substituting the value of $y_c$ in terms of $Q_L$, we obtain

$$Q_U = \frac{(1 + g_o)}{g_o\left(1 + \frac{g_o}{g_s}\right)\left(1 + \frac{1}{g_s}\right)\left(1 - \frac{g_o}{g_s}\right)} Q_L. \tag{1-12}$$

A plot of the ratio of $\frac{Q_U}{Q_L}$ is given as a function of $(SWR)_{o\ db}$ for different values of $(SWR)_{\infty\,db}$ in Fig. 1-4. Since we know $Q_L$, this determines $Q_U$. The values of $(SWR)_{o\ db}$ may be either positive or negative depending on whether $g_o$ is less or greater than unity. This may be determined by the phase curve.

If the phase curve is given by a curve of the shape shown in Fig. 1-5, it corresponds to a positive $(SWR)_{o\ db}$.

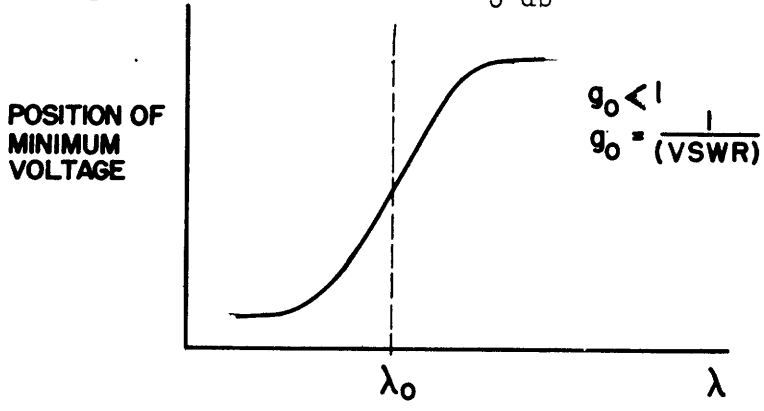


Fig. 1-5. Phase curve for $g_o < 1$.

If the phase is given by a curve of the shape shown in Fig. 1-6, it corresponds to a negative $(SWR)_{o\ db}$.

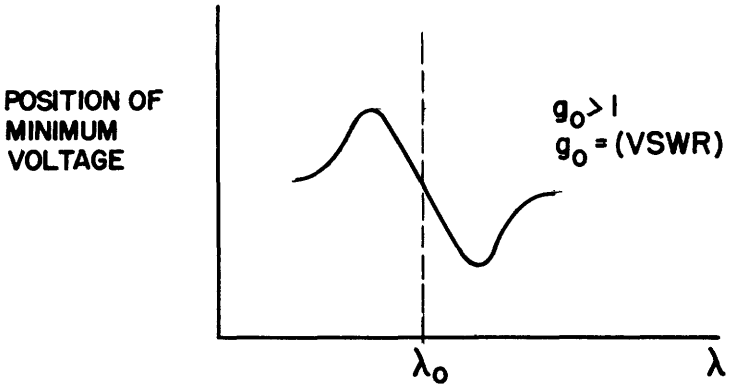


Fig. 1-6. Phase curve for $g_o > 1$.

Having determined the loaded Q, $Q_L$, from Eq. (1-10), one may calculate the normalized admittance by Eq. (1-4) writing

$$y_c = \frac{1 + g_o}{(1 + \frac{1}{g_s})(1 - \frac{g_o}{g_s})} Q_L \quad . \tag{1-13}$$

Using this equation we plot $\frac{y_c}{Q_L}$ as a function of $(SWR)_{o\ db}$ for different values of $(SWR)_{\infty\ db}$ in Fig. 1-7. From this family of curves, and our previous determination of $Q_L$, we may arrive at a value of $y_c$.

1.2. Q with No Series Loss. The problem of determining the various kinds of Q's is greatly simplified if the series loss can be neglected. In this case the determination is simplified since the $(SWR)_\infty$ is essentially infinite. From the top curve of Fig. 1-3 one may read the half-power points and thus determine $Q_L$ from Eq. (1-10).

The unloaded Q may be determined very simply by this method from the equation:

$$Q_U = Q_L(1 + \frac{1}{g_o}). \tag{1-14}$$

When the series conductance can be neglected, one may introduce a so-called external Q, $Q_E$, which is equal to $y_c$ in this case. One may

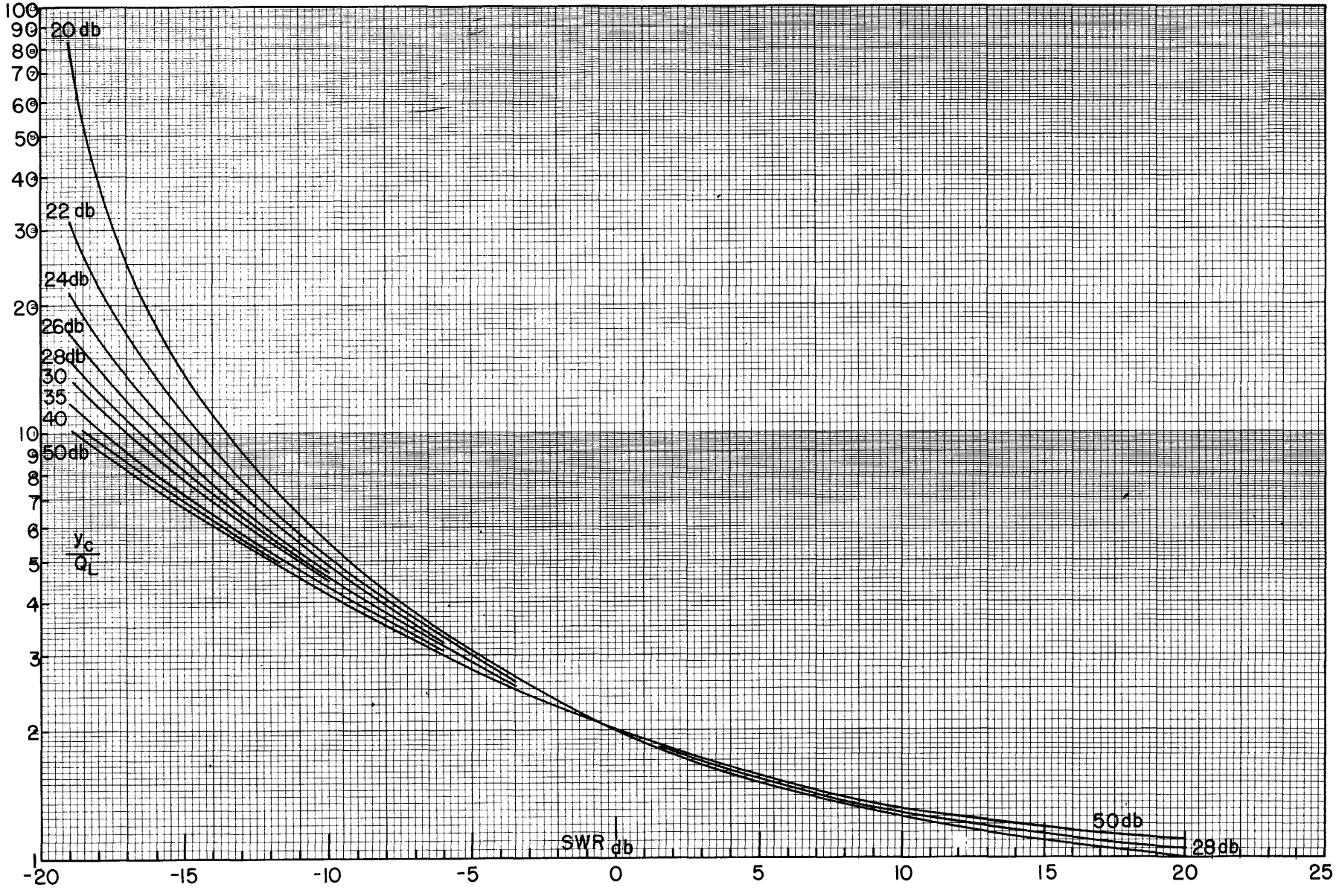


Fig. 1-7. The ratio of the normalized admittance to the loaded Q plotted as a function of the standing-wave ratio on resonance.

calculate this quantity

$$Q_E = y_c = Q_U g_o. \tag{1-15}$$

1.3. $Q_E$'s from the Slope of the Phase Curve. When the normalized cavity admittance $y_c$ is quite low, it is often difficult to measure it by the method given above. If, for example, $y_c$ is 5, the wavelength separation of the half-power points is enormous. There is, however, a convenient method of measuring low values of $y_c$. It is sufficient to measure the slope of the curve of minimum position vs. wavelength on resonance and the standing-wave ratio on resonance. Invariably for this case it will turn out that $g_p \ll 1$ so that it will be permissible on resonance to neglect the series resistance $\frac{1}{g_s}$. The circuit takes the form of Fig. 1-8.

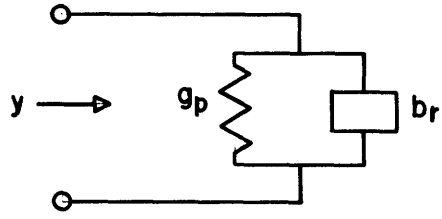


Fig. 1-8. Equivalent input circuit.

The normalized cavity susceptance $b_r$ is given by

$$b_r = y_c\left(\frac{\omega}{\omega_o} - \frac{\omega_o}{\omega}\right).$$

In the vicinity of resonance $b_r$ will be very small. We shall replace $b_r$ by $db_r$ and neglect all terms in $(db_r)^2$ in the following manipulations. Near resonance, the admittance is

$$y = g_p + jdb_r,$$

which leads to a reflection coefficient $\Gamma$:

$$\Gamma = \frac{1 - y}{1 + y} = \frac{1 - g_p - jdb_r}{1 + g_p + jdb_r}$$

$$\Gamma = \frac{(1 - g_p^2) - j2db_r}{(1 + g_p)^2} \quad . \tag{1-16}$$

The phase angle of the reflection coefficient is

$$d\theta = \frac{2db_r}{g_p^2 - 1} \quad . \tag{1-17}$$

The next step will be to find how the minimum position of the standing waves depends on $d\theta$ and $d\lambda$. The minimum position on resonance is given by

$$x = \frac{2n + 1}{4} \lambda_g + \frac{\theta \lambda_g}{4\pi} \tag{1-18}$$

where n is an integer and $\lambda_g$ is the guide wavelength, so that

$$\frac{dx}{d\lambda} = \frac{2n + 1}{4} \frac{d\lambda_g}{d\lambda} + \frac{\lambda_g}{4\pi} \frac{d\theta}{d\lambda} + \frac{\theta}{4\pi} \frac{d\lambda_g}{d\lambda}. \tag{1-19}$$

One notes that $\theta$ is $2\pi$ for a minimum shift of $\frac{\lambda_g}{2}$. The $\frac{2n + 1}{4}$ term represents an odd number of quarter wavelengths between the cavity and the point at which the phase measurements are being made. We evaluate this derivative at $\theta = 0$, $\lambda = \lambda_o$, $\lambda_g = \lambda_{go}$, using the relation $\frac{d\lambda_g}{d\lambda} = \left(\frac{\lambda_g}{\lambda}\right)^3$ and obtain

$$\left.\frac{dx}{d\lambda}\right|_{\theta=0} = \frac{2n + 1}{4} \left(\frac{\lambda_{go}}{\lambda_o}\right)^3 + \left.\frac{\lambda_{go}}{4\pi} \frac{d\theta}{d\lambda}\right|_{\theta=0} \tag{1-20}$$

We know

$$\left.\frac{d\theta}{d\lambda}\right|_{\theta=0} = \left.\frac{d\theta}{db_r}\right|_{\theta=0} \cdot \left.\frac{db_r}{d\lambda}\right|_{\theta=0} \tag{1-21}$$

But $\left.\frac{db_r}{d\lambda}\right|_{\theta=0}$ is simply $-\frac{2y_c}{\lambda_o}$ by definition of $b_r$, and $\left.\frac{d\theta}{db_r}\right|_{\theta=0}$ is given by Eq. (1-17). With these insertions in (1-20) and (1-21) we find upon simplifying

$$\left.\frac{dx}{d\lambda}\right|_{\theta=0} = \frac{2n + 1}{4}\left(\frac{\lambda_{go}}{\lambda_o}\right)^3 + \frac{y_c \lambda_{go}}{\pi(1 - g_p^2)\lambda_o}$$

whence

$$y_c = \pi(1 - g_p^2)\left[\frac{dx}{d\lambda}\Big|_{\theta=0}\left(\frac{\lambda_o}{\lambda_{go}}\right) - \frac{2n+1}{4}\left(\frac{\lambda_{go}}{\lambda_o}\right)^2\right] . \qquad (1\text{-}22)$$

Here $g_p$ is the reciprocal of the voltage standing-wave ratio on resonance; the $(1 - g_p^2)$ term usually is a very small correction for low $y_c$; $\frac{dx}{d\lambda}\Big|_{\theta=0}$ is simply the slope of the phase curve on resonance; $\frac{2n+1}{4}$ will be an odd multiple of $\frac{1}{4}$ and can usually be found by measuring the physical distance in guide wavelengths between the cavity and slotted section. The unloaded Q in this case is given by

$$Q_U = \frac{y_o}{g_p} . \qquad (1\text{-}23)$$

## Section 2. MEASUREMENT OF ELECTRIC FIELD

Two of the experimental quantities that may be measured pertaining to a microwave resonant cavity containing a gas discharge are the power incident on the cavity and the standing-wave pattern in the line leading to the cavity. It is necessary to relate these measurable quantities to the electric field and current densities in the cavity. This section will be concerned with the electric field only.

Three methods will be described. The first method presumes a knowledge of the field configuration within the cavity in question, which allows one to compute the relationship between electric field and stored energy. The second and third methods are applicable when the exact field configuration within the cavity are not easily calculated. The second method is adapted best for cavities for which $y_c > 100$, and the third method is best for cavities for which $y_c < 100$.

2.1. Simple Mode Cavities. The previous section has described means of measuring the various Q's of the cavity by means of standing-wave techniques. From the definition of the unloaded Q, $Q_U$, the power absorbed by the cavity may be related to the electromagnetic energy stored in the cavity. The power P absorbed by the cavity is related to the incident power $P_i$ by the relation,

$$P = P_i(1 - |\Gamma|^2) = P_i \frac{4\rho}{(1+\rho)^2}, \qquad (2\text{-}1)$$

where $\Gamma$ is the reflection coefficient of the cavity and $\rho$ is the voltage standing-wave ratio. The ratio $\frac{P}{P_i}$ plotted as a function of $(SWR)_{db}$ is shown in Fig. 2-1. By using the information thus far at our disposal, the stored energy U may be measured. It is therefore necessary to determine the relation between U and the electric field.

In general the stored energy may be expressed as

$$U = \eta E^2 \qquad (2\text{-}2)$$

where E is the rms magnitude of the electric field at an arbitrarily chosen reference point in the cavity and $\eta$ is a parameter which is fixed for a given mode of oscillation and given field reference point. From the relation,

$$U = CV^2,$$

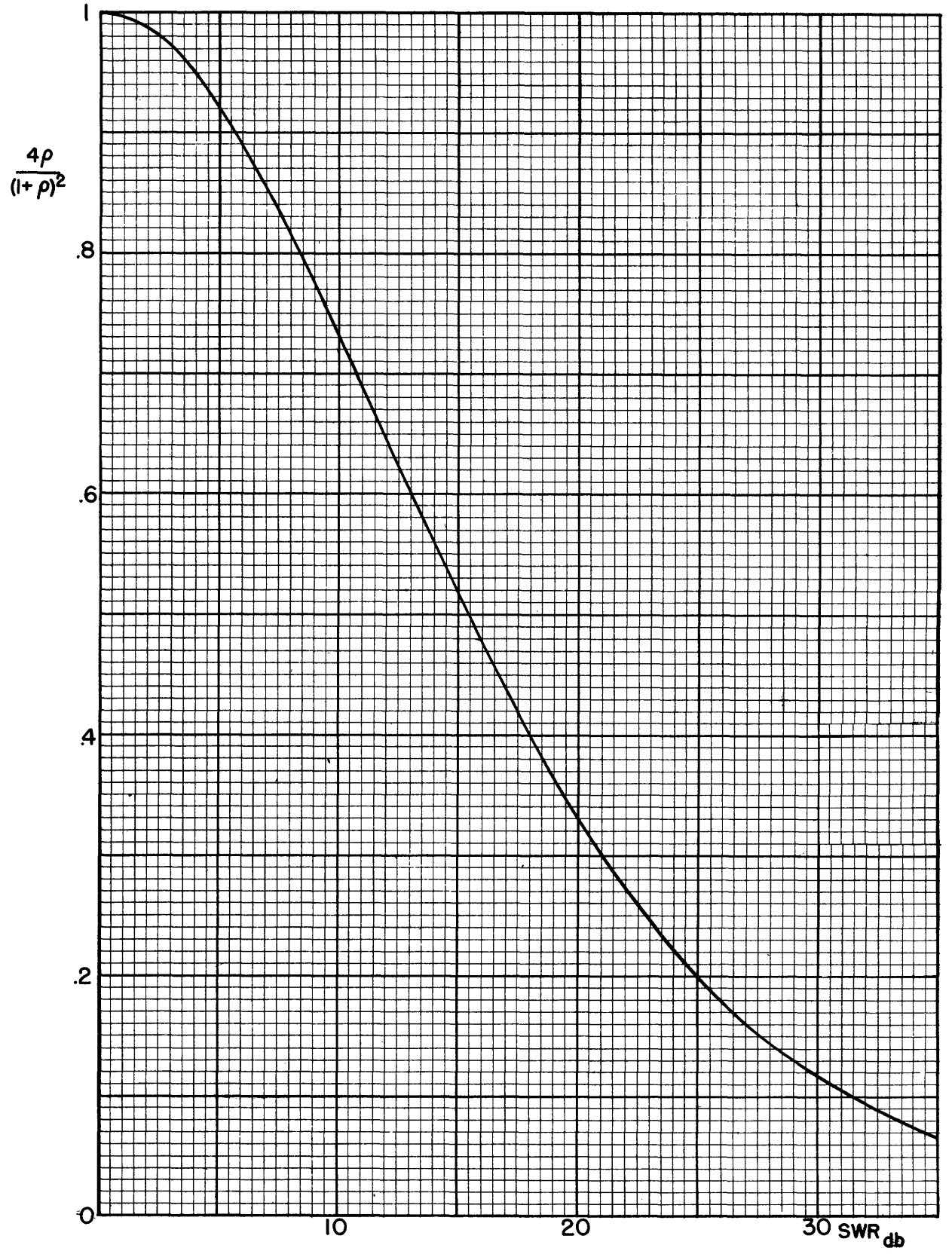


Fig. 2-1. Ratio of absorbed to incident power as a function of standing-wave ratio.

where C is the capacitance of a lumped-constant resonant circuit and V is the rms voltage across the capacity, the parameter $\eta$ may be seen to be a capacitance-like quantity, except that it is referred to the electric field instead of to the voltage.

By definition of $\eta$ and $Q_U$,

$$E = \sqrt{\frac{PQ_U}{\eta \omega}} \qquad (2\text{-}3)$$

Since P and $Q_U$ are known, it remains to compute $\eta$ for a given cavity. This calculation is illustrated below for the cylindrical $TM_{010}$-mode cavity, and the results for several other cavities are given in Table I. When the cavity has a complicated shape it is not feasible to compute $\eta$, but a method of measuring it is given below.

For the cylindrical $TM_{010}$-mode,

$$E_r = E_\theta = 0$$

$$E_z = \sqrt{2}\, E J_o\left(\frac{2.405\ r}{R}\right) e^{j\omega t} .$$

At the instant the electric field is a maximum the magnetic field (not given above) is zero, and the stored energy is

$$U = \tfrac{1}{2}\epsilon_o \int_o^R \left[\sqrt{2} E J_o\left(\frac{2.405\ r}{R}\right)\right]^2 2\pi r L\, dr,$$

where L is the length of the cavity, R its radius. The integration yields

$$U = 0.2695\ \epsilon_o V E^2 ,$$

where $\epsilon_o$ is the permittivity of free-space, and V the volume of the cavity = $\pi R^2 L$. Thus

$$\eta = 0.2695\ \epsilon_o V .$$

2.2. Tuning-Rate Method. For a cavity having a more complicated shape it is often difficult and sometimes impossible to compute $\eta$ accurately. For these cases an experimental procedure is given below for measuring the electric

TABLE I

| CAVITY | MODE | CONFIGURATION OF ELECTRIC FIELD | $\eta$ |
|---|---|---|---|
| CYLINDRICAL 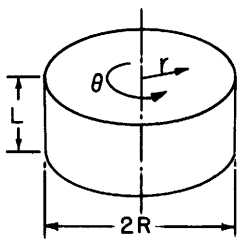  INDEX DIMENSION $\ell$ θ m R (r) n L (z) | TM | $E_z = \frac{E_{zmax.}}{J_\ell(x_{\ell m}\frac{r_{max.}}{R})} J_\ell(x_{\ell m}\frac{r}{R})\cos\ell\theta\cos\frac{n\pi}{L}z$<br>$E_r = -\frac{E_{zmax.}}{J_\ell(x_{\ell m}\frac{r_{max.}}{R})}\frac{n\pi R}{x_{\ell m}L} J_\ell'(x_{\ell m}\frac{r}{R})\cos\ell\theta\sin\frac{n\pi}{L}z$<br>$E_\theta = \frac{E_{zmax.}}{J_\ell(x_{\ell m}\frac{r_{max.}}{R})}\frac{n\pi R^2}{x_{\ell m}^2 L}\frac{J_\ell(x_{\ell m}\frac{r}{R})}{r}\sin\ell\theta\sin\frac{n\pi}{L}z$ | $\eta = \frac{U}{E_{zmax.}^2} = \frac{[1+\delta(\ell,0)][1+\delta(n,0)]\epsilon_0(\pi R^2 L)}{4J_\ell^2(x_{\ell m}\frac{r_{max.}}{R})} \times$<br>$\times\left\{\frac{1}{2}\left(\frac{n\pi R}{x_{\ell m}L}\right)^2\left[J_{\ell-1}^2(x_{\ell m})+J_{\ell+1}^2(x_{\ell m})\right]-J_{\ell-1}(x_{\ell m})J_{\ell+1}(x_{\ell m})\right\}$<br>$E_{zmax.}$ IS THE LARGEST rms. VALUE OF E IN THE z DIRECTION, AND OCCURS AT $r_{max.}$ THIS IS NOT NECESSARILY THE LARGEST FIELD WITHIN CAVITY. |
| | TE | $E_\theta = \frac{E_{\theta max.}}{J_\ell'(x'_{\ell m}\frac{r_{max.}}{R})} J_\ell'(x'_{\ell m}\frac{r}{R})\cos\ell\theta\sin\frac{n\pi}{L}z$<br>$E_r = \frac{E_{\theta max.}}{J_\ell'(x'_{\ell m}\frac{r_{max.}}{R})}\ell\frac{D}{x'_{\ell m}}\frac{J_\ell(x'_{\ell m}\frac{r}{R})}{r}\sin\ell\theta\sin\frac{n\pi}{L}z$ | $\eta = \frac{U}{E_{\theta max.}^2} = \frac{[1+\delta(\ell,0)]\epsilon_0(\pi R^2 L)}{8J_\ell'^2(x'_{\ell m}\frac{r_{max.}}{R})} \times$<br>$\times\left\{J_{\ell-1}^2(x'_{\ell m})-J_{\ell-2}(x'_{\ell m})J_\ell(x'_{\ell m})+J_{\ell+1}^2(x'_{\ell m})-J_\ell(x'_{\ell m})J_{\ell+2}(x'_{\ell m})\right\}$<br>$E_{\theta max.}$ IS THE LARGEST rms. VALUE OF E IN THE θ DIRECTION, AND OCCURS AT $r_{max.}$ THIS IS NOT NECESSARILY THE LARGEST FIELD WITHIN CAVITY. |
| RECTANGULAR 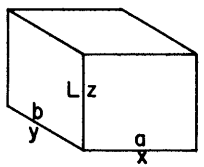  INDEX DIMENSION $\ell$ a (x) m b (y) n L (z) | TM $\ell,m>0$ | $E_z = E_{zmax.}\sin\frac{\ell\pi}{a}x\sin\frac{m\pi}{b}y\cos\frac{n\pi}{L}z$<br>$E_x = -E_{zmax.}\frac{(\ell/a)(n/L)}{(\ell/a)^2+(m/b)^2}\cos\frac{\ell\pi}{a}x\sin\frac{m\pi}{b}y\sin\frac{n\pi}{L}z$<br>$E_y = -E_{zmax.}\frac{(m/b)(n/L)}{(\ell/a)^2+(m/b)^2}\sin\frac{\ell\pi}{a}x\cos\frac{m\pi}{b}y\sin\frac{n\pi}{L}z$ | $\eta = \frac{U}{E_{zmax.}^2} = \frac{\epsilon_0 abL}{8}\left\{1+\delta(n,0)+\frac{[1-\delta(n,0)](n/L)^2}{[(\ell/a)^2+(m/b)^2]}\right\}$<br>$E_{zmax.}$ IS THE LARGEST rms. VALUE OF E IN z DIRECTION, BUT IS NOT NECESSARILY THE LARGEST FIELD WITHIN CAVITY. |
| | TE m,n>0 | $E_x = E_{xmax.}\cos\frac{\ell\pi x}{a}\sin\frac{m\pi y}{b}\sin\frac{n\pi z}{L}$<br>$E_y = E_{xmax.}\frac{b}{a}\frac{\ell}{m}\sin\frac{\ell\pi x}{a}\cos\frac{m\pi y}{b}\sin\frac{n\pi z}{L}$ | $\eta = \frac{U}{E_{xmax.}^2} = \frac{\epsilon_0 abL}{8}\left\{1+\left(\frac{b}{a}\frac{\ell}{m}\right)^2+\delta(\ell,0)\right\}$<br>$E_{xmax.}$ IS THE LARGEST rms. VALUE OF E IN x DIRECTION, BUT IS NOT NECESSARILY THE LARGEST FIELD WITHIN CAVITY. IF $\ell>0$, m=0, ONLY $E_y$ EXISTS. THIS CASE IS COVERED BY A ROTATION OF 90° IN x,y PLANE. |

$x_{\ell m}$ IS $m^{th}$ ROOT OF $J_\ell(x)$

$x'_{\ell m}$ " " " " $J'_\ell(x)$

$J'_\ell(x_{\ell m}r/R) = \frac{d\,J_\ell(x_{\ell m}r/R)}{d(x_{\ell m}r/R)}$

$\delta(p,0) = 1$ WHEN $p=0$

$= 0$ WHEN $p\neq 0$

field when the cavity admittance $y_c > 100$. Suppose a small metallic body of volume dv is physically inserted into the cavity in the region of maximum electric field. An easy way to accomplish this is to insert a small metallic plug of A a distance $d\delta$ into the cavity. In this case $dv = Ad\delta$. The effect of this insertion will be that the cavity's resonant wavelength $\lambda$ will be shifted a small amount $d\lambda$. It is clear that $d\lambda/dv$ is a quantity easily measured experimentally. The rms electric field E is then given directly by

$$E^2 = \frac{d\lambda}{dv} \frac{Q_U P}{\pi} \sqrt{\frac{\mu_o}{\epsilon_o}} \quad . \tag{2-4}$$

Here E is in volts/meter, $\lambda$ in meters, v in meters$^3$, P in watts, and $\sqrt{\mu_o/\epsilon_o} = 377$ ohms.

Before deriving Eq. (2-4) it will be interesting to apply it to a simple case showing that it is equivalent to Eq. (2-3). Consider a reentrant cavity with inductance L and capacity C in which the capacity C is that of parallel plates of area A and spacing $\delta$. The wavelength of the cavity is

$$\lambda = 2\pi c\sqrt{LC} \tag{2-5}$$

where c is the velocity of light. We imagine an experiment in which we introduce a sheet of metal of area A and thickness $d\delta$ between the parallel plates of the condenser C. The wavelength $\lambda$ will change by an amount $d\lambda$. Dividing Eq. (2-5) into its differential we find

$$\frac{d\lambda}{\lambda} = \frac{dC}{2C} \quad . \tag{2-6}$$

Inasmuch as the capacity is $\epsilon_o A/\delta$, the change in capacity is

$$dC = -\frac{\epsilon_o A}{\delta^2} d\delta = \frac{\epsilon_o dv}{\delta^2} \tag{2-7}$$

the change of sign coming from the fact that positive dv represents a decrease in volume of the capacitor. Inserting Eq. (2-7) into Eq. (2-6) and solving for C, we obtain

$$C = \frac{\lambda}{2d\lambda} \cdot \frac{\epsilon_o dv}{\delta^2} \quad . \tag{2-8}$$

For parallel plates, by definition of $\eta$ we have $\eta = C\delta^2$. Hence, from Eq. (2-8) we obtain

$$\eta = \frac{dv}{d\lambda}\frac{\epsilon_o \lambda}{2} . \tag{2-9}$$

But

$$\frac{\epsilon_o \lambda}{2} = \frac{\epsilon_o (2\pi f)\lambda}{2\omega} = \frac{\epsilon_o \pi c}{\omega} = \frac{\epsilon_o \pi}{\omega\sqrt{\mu_o \epsilon_o}} = \frac{\pi}{\omega}\sqrt{\frac{\epsilon_o}{\mu_o}}$$

so that

$$\eta = \frac{dv}{d\lambda} \cdot \frac{\pi}{\omega}\sqrt{\frac{\epsilon_o}{\mu_o}} . \tag{2-10}$$

It is evident from (2-10) that Eq. (2-4) has been shown to be of the form

$$E^2 = \frac{Q_U P}{\omega \eta} = \frac{d\lambda}{dv}\frac{Q_U P}{\pi}\sqrt{\frac{\mu_o}{\epsilon_o}}$$

in agreement with Eq. (2-3).

For completeness we include a general derivation of Eq. (2-4). The variation principle for electromagnetic problems, analogous to Hamilton's principle in mechanics, is that

$$\tfrac{1}{2}\int_{\text{time}}\int_{\text{volume}} (\epsilon \mathcal{E}^2 - \mu H^2)\, dv\, dt \tag{2-11}$$

have a stationary value of zero. If one uses the induction law

$$\text{curl } \mathcal{E} + \frac{\partial B}{\partial t} = 0$$

and assumes a sinusoidal time variation with frequency $\omega$, (2-11) can be put in the form

$$\frac{\epsilon_o}{4}\int\left(E_o^2 - \frac{c^2}{\omega^2}(\text{curl } E_o)^2\right)dv = 0 \tag{2-12}$$

in which the integration over time has been performed. Here $E_o(x,y,z)$ is the peak value of the electric field. From Eq. (2-12) one finds

$$\left(\frac{\lambda}{2\pi}\right)^2 = \frac{c^2}{\omega^2} = \frac{\int E_o^2 dv}{\int_{vol.} (\text{curl } E_o)^2 dv} \qquad (2\text{-}13)$$

which is the equation for the wavelength of a cavity in terms of integrals over the electric field and its curl. Let us perturb the cavity slightly by a local variation in the volume, $\Delta v$, in a region of the cavity where B and hence curl $E_o$ are small. At this place $E_o(x,y,z)$ will have its maximum value. The wavelength will change by an amount $\Delta\lambda$, the numerator by an amount $E_1^2 \Delta v$ where $E_1$ is the average value over $\Delta v$, and the denominator will not change since curl $E_o$ is small in the region of $\Delta v$. Thus

$$2\left(\frac{\lambda}{2\pi}\right)\frac{\Delta\lambda}{2\pi} = \frac{E_1^2 \Delta v}{\int_{vol.} (\text{curl } E_o)^2 dv} \qquad (2\text{-}14)$$

Dividing Eq. (2-14) by Eq. (2-13) and letting $\Delta\lambda \rightarrow d\lambda$, $\Delta v \rightarrow dv$, one obtains upon solving for $E_1^2$:

$$E_1^2 = \frac{2}{\lambda}\frac{d\lambda}{dv}\int E_o^2 dv \ .$$

One recognizes that

$$\int E_o^2 dv = \frac{2U}{\epsilon_o}$$

where U is the total stored energy. With this substitution

$$E_1^2 = \frac{2}{\lambda}\frac{d\lambda}{dv}\frac{2U}{\epsilon_o} \ .$$

Ordinarily one measures U by measuring P, the power absorbed by the cavity. By definition of $Q_U$, the unloaded Q, we have

$$U = \frac{Q_U P}{\omega} \ ,$$

whence

$$E_1^2 = \frac{2}{\lambda}\frac{d\lambda}{dv}\frac{2Q_U P}{\epsilon_o \omega},$$

which becomes after simplification

$$E_1^2 = \frac{2}{\pi}\frac{d\lambda}{dv} Q_U P \sqrt{\frac{\mu_o}{\epsilon_o}}.$$

In terms of rms fields $E = E_1/\sqrt{2}$

$$E^2 = \frac{d\lambda}{dv}\frac{Q_U P}{\pi}\sqrt{\frac{\mu_o}{\epsilon_o}} \qquad (2\text{-}4)$$

which completes the derivation of Eq. (2-4).

2.3. Four-Terminal Network Method. When the resonant region is coupled very strongly to the transmission line the cavity concept is no longer applicable. In this case it is convenient to use the 4-terminal network method described in Sec. 3 where the reader will note that all the necessary equivalent circuit parameters are experimentally evaluated. A slight extension of Eq. (3-17) gives us the formula for the rms electric field:

$$E^2 = \frac{a^2}{\delta^2} V_o^2 = \sqrt{\frac{\mu_o}{\epsilon_o}} \cdot \frac{\lambda_o}{\lambda_g} \cdot \left|\frac{dx}{d\delta}\right| \frac{(1 - g^2)}{S_1} Y_o V_o^2 \qquad (2\text{-}15)$$

in the notation of Sec. 3. In Eq. (2-5) $V_o$ is the rms voltage in the transmission line at the reference plane AA' of Fig. (3-5) and is given by

$$V_o^2 = PZ_o h .$$

Here P is the power absorbed by the load in watts,
$Z_o$ is the characteristic impedance of the transmission line,
h is the VSWR when AA' is at a maximum of the standing-wave pattern and is 1/VSWR when AA' is at a minimum of the standing-wave pattern.

## Section 3. THE MEASUREMENT OF COMPLEX CONDUCTIVITY

Let a high-frequency electric field $E_o e^{j\omega t}$ be impressed on an ionized gas. In addition to the displacement current density $J_d = j\omega\epsilon_o E_o e^{j\omega t}$ there is an electron current density $J_e$ with two components: $J_r$, the real electron current density in phase with the field, and $J_i$, the reactive electron current density out of phase with the field, so that

$$J_e = J_r + jJ_i .$$

The complex conductivity $\sigma_c$ is defined by

$$\sigma_c = \frac{J_e}{E} = \frac{J_r}{E} + j\frac{J_i}{E} = \sigma_r + j\sigma_i .$$

Thus $\sigma_c$, a property of the gas, and $\epsilon_o$, a property of empty space, completely characterize the space. This is the viewpoint adopted in this chapter.

An alternative and equivalent viewpoint is to characterize the ionized medium by a complex permittivity $\epsilon_c = \epsilon_r - j\epsilon_i$ in which the effect of the real conductivity is included in $\epsilon_i$. According to this alternative viewpoint, Maxwell's equation curl $H = \dot{D} + J$ becomes

$$\text{curl } H = j\omega\left(\epsilon_r - j\epsilon_i\right)E_o e^{j\omega t} , \qquad (3\text{-}1)$$

whereas in terms of the first viewpoint

$$\text{curl } H = (j\omega\epsilon_o + \sigma_r + j\sigma_i)E_o e^{j\omega t}$$

$$= j\omega\left[(\epsilon_o + \frac{\sigma_i}{\omega}) - j(\frac{\sigma_r}{\omega})\right] E_o e^{j\omega t} . \qquad (3\text{-}2)$$

Comparison of Eq. (3-1) and Eq. (3-2) shows that

$$\epsilon_r = \epsilon_o + \frac{\sigma_i}{\omega}$$

$$\epsilon_i = \frac{\sigma_r}{\omega} .$$

The complex dielectric coefficient is thus

$$K_c = \frac{\epsilon_c}{\epsilon_o} = \left(1 + \frac{\sigma_i}{\epsilon_o \omega}\right) - j \frac{\sigma_r}{\omega \epsilon_o} \qquad (3\text{-}3)$$

so that if one prefers, he can convert $\sigma_r$ and $\sigma_i$ into the equivalent complex dielectric constant.

3.1. Conductivity and Admittance. We can allow the high-frequency electric field existing in a driven microwave cavity to maintain a gas discharge within the cavity. An alternative procedure is to maintain the discharge with d-c or low-frequency electric field and use the microwaves as a low-level probe. In either case one measures standing-wave ratio and phase in the input line and converts these into values for the conductance and susceptance of the discharge. The next two parts of this section are concerned with the detailed procedure for accomplishing this. One finds that the conductance and susceptance of the discharge are expressible in terms of integrals over $\sigma_r$ and $\sigma_i$. This relationship is explored in the last part of this section.

3.2. Cavity Method of Determining G and B. When the discharge is located at the center of a cavity resonator whose $y_c$ is greater than 100 it is convenient to use cavity theory to determine G and B. The cavity containing the discharge is used as a load at the end of a microwave transmission line. It will be possible to measure standing waves in the transmission line and determine from them the actual value of G and B of the discharge.

Let us draw an equivalent circuit for the cavity and then determine experimentally certain parameters of that circuit. An empty microwave cavity with an input loop is well represented by the circuit of Fig. 3-1. Here $G_s$

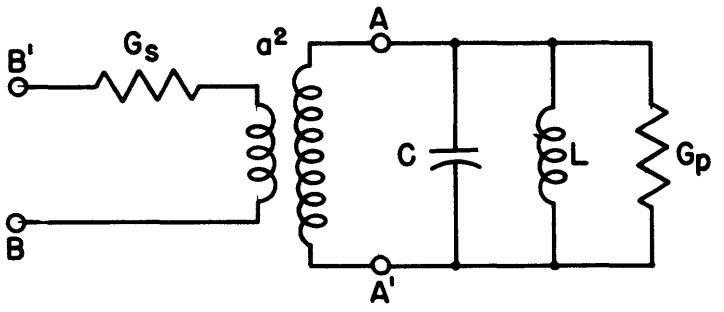


Fig. 3-1. Equivalent circuit for microwave cavity.

is the series loss in the transmission line; $a^2$ is the admittance transformer ratio of the ideal transformer; C,L, and $G_p$ are respectively the actual capacitance, inductance, and conductance of the cavity. We shall determine some of these constants by using the empty cavity as a load while making certain standing-wave measurements in the transmission line.

One first measures $y_c$ and $Q_U$ by the method described in the first section of this report. It will be advantageous to arrange the coupling loop so that $y_c < Q_U$. In fact $y_c$ may well be as low as 100 for certain measurements. In taking the measurements one records the phase of the standing-wave pattern as well as the amplitude. Next one determines a reference point in the slotted section which is exactly an integral number of half wavelengths from the cavity terminal AA'. This is best done by physically shorting the cavity with a substantial metallic conductor across the region which would normally have the maximum electric field, taking care not to place the shorting conductor too near the input loop. Any minimum position of the standing-wave pattern is then an integral number of half wavelengths from AA'. The voltage standing-wave ratio obtained is $G_s/Y_o$. One should determine this reference point in the slotted section as a function of frequency. The angular resonant frequency $\omega_o$ of the cavity is most accurately defined as that at which the reference point determined above lies exactly $\lambda_g/4$ from the minimum position recorded during the Q-measurement. The shorting bar is then removed. The circuit of Fig. 3-1 is equivalent to that of Fig. 3-2, in which all admit-

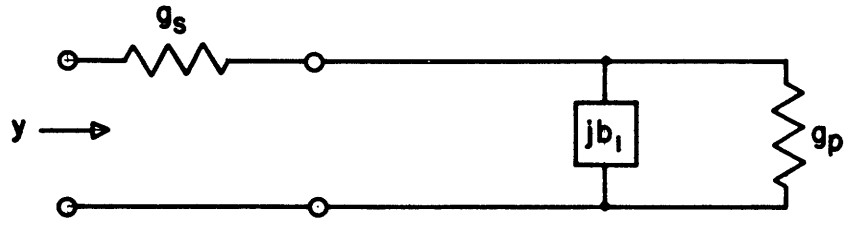


Fig. 3-2. Normalized equivalent circuits.

tances and resistances have been normalized with respect to $Y_o$, the characteristic admittance of the line. In fact

$$g_s = \frac{G_s}{Y_o}$$

is the normalized series conductance, and $b_1$ the normalized susceptance is given by

$$b_1 = \frac{\omega a^2 C}{Y_o} - \frac{a^2}{\omega Y_o L}$$

$$= \frac{a^2}{Y_o}\sqrt{\frac{C}{L}}\left(\frac{\omega}{\omega_o} - \frac{\omega_o}{\omega}\right)$$

$$= \frac{a^2\omega_o C}{Y_o}\left(\frac{\omega}{\omega_o} - \frac{\omega_o}{\omega}\right)$$

$$= y_c\left(\frac{\omega}{\omega_o} - \frac{\omega_o}{\omega}\right) \tag{3-4}$$

where $\omega_o = 1/\sqrt{LC}$. The normalized conductance $g_p$ is given by

$$g_p = \frac{a^2 G_p}{Y_o} = \frac{y_c}{Q_U} = \frac{a^2\omega_o C}{Y_o Q_U}. \tag{3-5}$$

In the above equations the well-known relations

$$y_c = \frac{a^2}{Y_o}\sqrt{\frac{C}{L}} = \frac{a^2\omega_o C}{Y_o} \tag{3-6}$$

and

$$Q_U = \frac{1}{G_p}\sqrt{\frac{C}{L}} = \frac{\omega_o C}{G_p} \tag{3-7}$$

have been used. We have already measured certain standing-wave ratios, $y_c$, and $Q_U$ so that $g_s$, $b_1$, and $g_p$ are known quantities. It is unfortunately necessary to determine the actual value of $G_p$. From Eq. (3-7) it is apparent that

$$G_p = \frac{\omega_o C}{Q_U} \tag{3-8}$$

so that, if the capacity of the cavity is known, we know $G_p$. In certain cases as in the examples of Sec. 2.1, it is possible to compute the capacity. The capacity C is simply $\eta\delta^2$ in the notation of that section.

An alternative procedure applies when it is not possible to compute the capacity. One must then make a measurement of the rate at which

the cavity wavelength $\lambda$ changes as one inserts a small tuning plug into the region of maximum electric field as has been described in Sec. 2. It will be recalled that the result found there for the rms electric field is

$$E^2 = \frac{d\lambda}{dv} \frac{Q_U P}{\pi} \sqrt{\frac{\mu_o}{\epsilon_o}} .$$

If it is possible to assume that the electric field is uniform over a gap of width $\delta$, then $E = V/\delta$ and $P = V^2 G_p$ where V is the rms voltage across the gap. Inserting these relations in the last equation and solving for $G_p$, one obtains

$$G_p = \frac{\pi}{\frac{d\lambda}{dv} Q_U \sqrt{\frac{\mu_o}{\epsilon_o}} \delta^2} . \qquad (3\text{-}9)$$

We now have determined all the necessary cavity parameters and may introduce a gas discharge into the cavity in order to measure G and B of the discharge. The equivalent circuit is that of Fig. 3-3. The discharge has

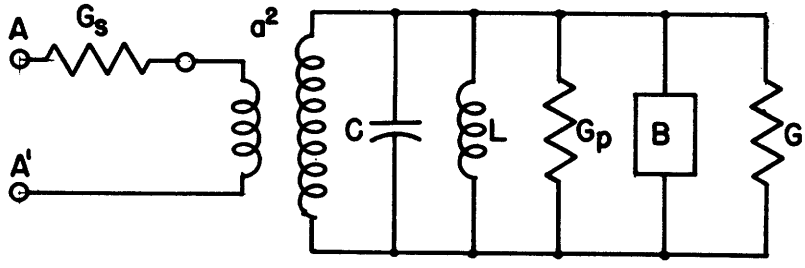


Fig. 3-3. Equivalent circuit with discharge.

been physically placed in the region of maximum electric field within the cavity so that its conductance and susceptance are in parallel with the terminals of the cavity. Figure 3-3 is equivalent to that of Fig 3-4, where all admittances are normalized.

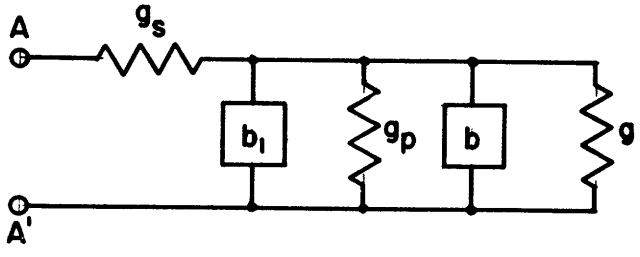


Fig. 3-4. Normalized equivalent circuit with discharge.

A measurement of standing-wave ratio and phase referred to the reference terminals $AA'$ determines uniquely b and g inasmuch as $g_s$, $b_1$, and $g_p$ are known. It is possible to write formulas for b and g in terms of the standing-wave ratio and phase at $AA'$ but these are so complicated that in practice it is much easier to use an impedance chart. It is often not permissible to neglect $g_s$.

Since

$$g = \frac{a^2 G}{Y_o}$$

and

$$b = \frac{a^2 B}{Y_o}$$

whereas

$$g_p = \frac{a^2 G_p}{Y_o} ,$$

it is evident that

$$\frac{g}{G} = \frac{b}{B} = \frac{g_p}{G_p} \tag{3-10}$$

so that using Eq. (3-8) and Eq. (3-5) we have

$$G = \frac{g}{g_p} G_p = g \cdot \frac{Q_U}{y_c} \frac{\omega_o C}{Q_u} = \frac{g\omega_o C}{y_c} \tag{3-11}$$

and similarly

$$B = \frac{b\omega_o C}{y_c} . \tag{3-12}$$

If one substitutes Eqs. (3-9) and (3-5) into Eq. (3-10) one obtains

$$G = \frac{g\pi}{y_c \frac{d\lambda}{dv} \sqrt{\frac{\mu_o}{\epsilon_o}}\, \delta^2} \tag{3-13}$$

and

$$B = \frac{b\pi}{y_c \frac{d\lambda}{dv} \sqrt{\frac{\mu_o}{\epsilon_o}}\, \delta^2} \quad . \tag{3-14}$$

Equations (3-11) and (3-12) are entirely equivalent to Eqs. (3-13) and (3-14).

3.3. Four-Terminal Network Method. In the case where the $y_c$ of the cavity is very low, of the order of 20, it is not accurate to apply cavity theory because of the complications introduced by other modes of the cavity. As a matter of fact, the discharge need not be located in a cavity at all. In this case there is an accurate method of measuring G and B of the discharge subject to the restriction that the region of the discharge is small compared to a wavelength.

Let the discharge form in some fashion a load on a transmission line. Let AA' be terminals located at an arbitrary position in the transmission line. Let CC' be the terminals at the discharge. It is permissible to take terminals at AA' because the transmission line supports but one mode of propagation. At CC' we have terminals because the discharge region is small compared to a wavelength. We thus have a four-terminal network as in Fig. 3-5. We have included the series loss in the transmission line as

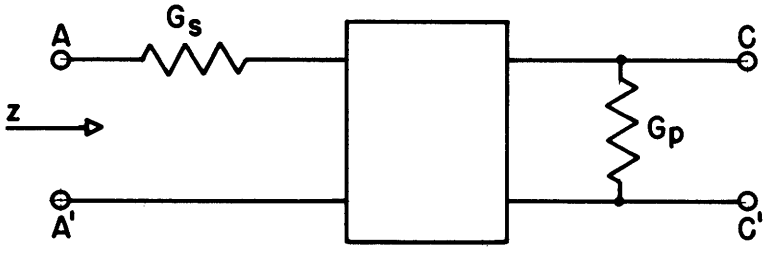


Fig. 3-5. Four-terminal network.

$G_s$ and the shunt loss in the walls of the cavity as a parallel conductance $G_p$. The box is composed of reactive elements. Of the many possible three-element reactive circuits to fit into the box that of Fig. 3-6 recommends itself. $X_1$ and $B_1$ are reactive elements to be determined and $a^2$ is the

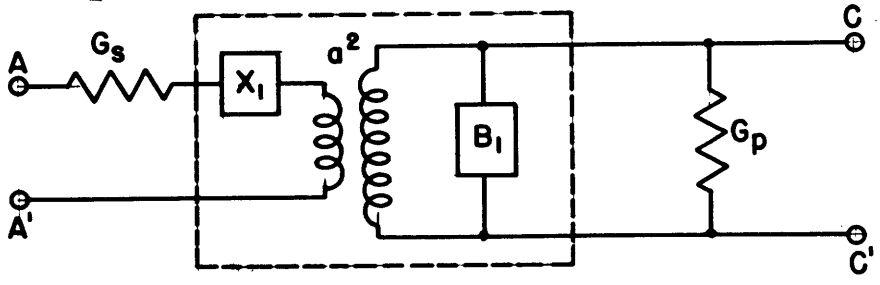


Fig. 3-6. Network with equivalent reactive elements.

admittance transformer ratio of an ideal transformer.

There is an experimental procedure for determining these parameters. We short CC' and measure the standing waves in the slotted section as a function of frequency. We then open CC' and repeat the measurements. It is best to choose AA' at the place where the minimum position with CC' shorted is exactly $\lambda_g/4$ away from the minimum position with CC' open. This procedure defines an angular frequency $\omega_o$ and the most convenient position for AA'. The fact that AA' is a minimum when CC' is shorted means that $X_1 = 0$. The fact that AA' is $\lambda_g/4$ away from a minimum when CC' is open means that $B_1 = 0$ also. When $\omega = \omega_o$ and with AA' chosen properly we have the circuit of Fig. 3-7. All that remains is to determine $G_s$, $G_p$ and $a^2$. $G_s/Y_o$ is the

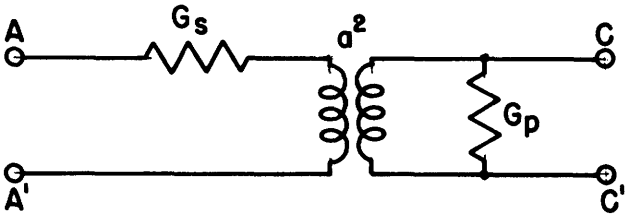


Fig. 3-7. Circuit simplified by correct choice of reference plane and frequency.

voltage standing-wave ratio obtained when CC' is shorted. $Y_o/G_s + Y_o/a^2G_p$ is the voltage standing-wave ratio obtained when CC' is opened.

The separate experimental determination of $a^2$ is necessary. We must look in detail at the physical structure of the points represented by CC'. These are the two actual posts across which the glow discharge is created. Let us presume them to be of parallel-plate structure as in Fig. 3-8. We shall add a known additional capacity across CC' and note the

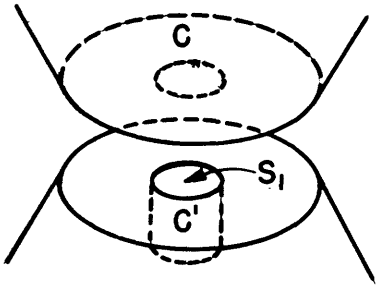


Fig. 3-8. Parallel-plate structure showing movable plug $S_1$.

impedance change at AA'. There are several ways in which this may be accomplished. One might, for example, add a small block of dielectric whose constant is known between CC' and compute the capacity added. As a second method one might place a thin disk of metal on one of the plates thereby

changing the effective separation and hence the capacity by a known amount. These methods both have the disadvantage that one makes a finite change in the capacity, thereby slightly distorting the field configuration. The particular method described below allows one to determine $a^2$ by means of an infinitesimal variation in capacity. It is quite similar to the procedure used in Sec. 2.2 and 2.3 to measure the electric field.

Figure 3-8 shows terminals CC' in the center of the parallel-plate region. The flat end of a movable metal plug is a small area $S_1$ in the center of the parallel-plate region. In its normal position the plug is flush to the surface of one of the parallel plates. Suppose the plug is inserted an infinitesimal distance $d\delta$. The additional capacity across CC' is $\epsilon_o S_1 d\delta/\delta^2$ where $\delta$ is the spacing of the gap. The original capacity of the parallel-plate region forms part of $X_1$ and is exactly cancelled by inductive elements since $X_1 = 0$. Neglecting $Y_o/G_s$ which is small compared to $Y_o/a^2G_p$ the equivalent circuit at AA' is that of Fig. 3-9.

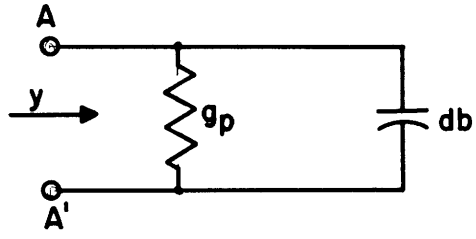


Fig. 3-9. Equivalent circuit when infinitesimal capacity is added at CC'.

From this figure

$$y = g_p + jdb$$

where

$$g_p = \frac{a^2 G_p}{Y_o}$$

and

$$db = \frac{a^2}{Y_o} \frac{\omega \epsilon_o S_1 d\delta}{\delta^2} . \qquad (3\text{-}15)$$

The voltage reflection coefficient

$$\Gamma = \frac{1 - y}{1 + y}$$

has a phase angle given by

$$d\theta = \frac{-2db}{1 - g_p^2} .$$

An infinitesimal insertion of the plug produces an admittance db. The corresponding phase angle $d\theta$ is closely related to the shift dx in the minimum position out in the transmission line. The ratio $dx/d\delta$ is measurable and is a measure of $a^2$, as will be shown. One has

$$\frac{dx}{d\delta} = \frac{dx}{d\theta} \cdot \frac{d\theta}{db} \cdot \frac{db}{d\delta}$$

$$= \frac{\lambda_g}{4\pi} \cdot \frac{-2}{1 - g_p^2} \cdot \frac{\omega a^2}{Y_o} \frac{\epsilon_o S_1}{\delta^2} \qquad (3\text{-}16)$$

whence

$$a^2 = \frac{2\pi}{\lambda_g} \left|\frac{dx}{d\delta}\right| \frac{(1 - g_p^2)\delta^2 Y_o}{\epsilon_o S_1 \omega}$$

$$= \sqrt{\frac{\mu_o}{\epsilon_o}} \cdot \frac{\lambda_o}{\lambda_g} \cdot \left|\frac{dx}{d\delta}\right| \frac{(1 - g_p^2)\delta^2 Y_o}{S_1} \qquad (3\text{-}17)$$

where

$\sqrt{\mu_o/e_o}$ = 377 ohms,

$\lambda_o$ = free-space wavelength,

$\lambda_g$ = guide wavelength,

$dx/d\delta$ = slope of the minimum-position vs. plug-insertion curve evaluated at the point where the plug is flush. All measurements at $\omega = \omega_o$.

$g$ = $a^2 G_o/Y_o$ = 1/VSWR when CC' is open circuited

$\delta$ = spacing of parallel plates,

$S_1$ = area of plug inserted,

$Y_o$ = characteristic admittance of the transmission line at AA' in reciprocal ohms.

All the necessary parameters of the circuit have been determined. Impedance measurements at AA' in Fig. 3-7 will thus give exactly the value of any impedance added across CC'.

3.4. Determination of $\sigma_r$ and $\sigma_i$. If one knows G and B for the gas discharge, one is in a position to compute $\sigma_r$ and $\sigma_i$ for the ionized medium. The method of doing this will depend on the geometry of the discharge and the way the electron concentration varies in space. This is a difficult problem and in practice one chooses the simplest possible geometric arrangement of the discharge. An example will be given.

Suppose we have a discharge which is between circular parallel plates of radius $r_o$ and spacing $\delta$ (Fig. 3-10). The electron concentration

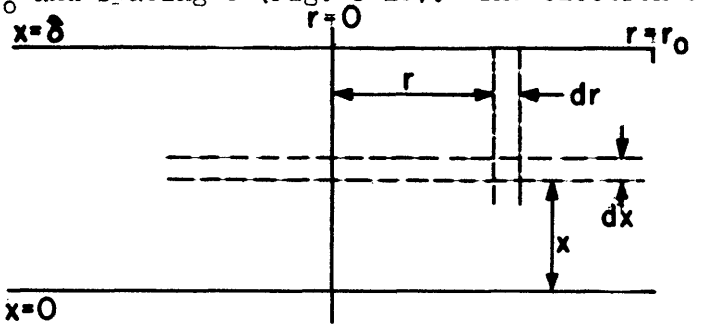


Fig. 3-10. Cross section of gas discharge between parallel plates.

will in general be a function of x and r. For simplicity we consider the electron concentration to be independent of r for $0 \leq r \leq r_o$ and to be zero for $r > r_o$. For $r < r_o$ then, the electron concentration is a function of x alone. Since $\delta$ is small compared to a wavelength, the current will be continuous across the gap if we include both electron current and displacement current. Fringing fields will be neglected which means that the equipotentials are parallel. We are justified therefore in the following computation of impedance.

The admittance associated with a slab of thickness dx is

$$\frac{\pi r_o^2 \left[\sigma_r(x) + j(\sigma_i(x) + \omega\epsilon_o)\right]}{dx}$$

where the $j\omega\epsilon_o$ term is the admittance of empty space and is related to the displacement current density. The impedance of the slab is

$$\frac{dx}{\pi r_o^2 \left[\sigma_r(x) + j(\sigma_i(x) + \omega\epsilon_o)\right]}$$

so that the impedance of the whole gap is

$$Z = \int_0^{\delta} \frac{dx}{\pi r_o^2 \left[\sigma_r(x) + j(\sigma_i(x) + \omega\epsilon_o)\right]} .$$

Actually

$$Z = \frac{1}{Y} = \frac{1}{G + jB'} .$$

In measuring G and B experimentally, however, we have automatically subtracted out a susceptance $B_c$ equal to that of the condenser before the discharge. Therefore

$$B = B' - B_c$$

or

$$B' = B + B_c$$

where

$$B_c = \frac{\pi r_o^2 \omega\epsilon_o}{\delta} .$$

Then

$$\frac{1}{G + j(B + B_c)} = \int_0^{\delta} \frac{dx}{\pi r_o^2 \left[\sigma_r(x) + j(\sigma_i(x) + \omega\epsilon_o\right]} \qquad (3\text{-}9)$$

gives the relationship between the measured values of G, B and $\sigma_r$, $\sigma_i$. Unfortunately the functional form of $\sigma_r(x)$ and $\sigma_i(x)$ must be independently derived from kinetic theory. One might expect $\sigma_r$ to be more or less proportional to G, and $\sigma_i$ to be more or less proportional to B. This turns out not to be the case. In the limit where

$$\sigma_r << \omega\epsilon_o$$

and

$$\sigma_i << \omega\epsilon_o ,$$

certain simplifications result in the formulas

$$G = \frac{\pi r_o^2}{\delta^2} \int_o^\delta \sigma_r(x)dx \qquad (3\text{-}20)$$

and

$$B = \frac{\pi r_o^2}{\delta^2} \int_o^\delta \sigma_i(x)dx \qquad (3\text{-}21)$$

But in almost all cases it is impossible to justify these assumptions and Eq. (3-19) must be applied.

## Section 4. TECHNIQUES FOR STUDYING TRANSIENT PHENOMENA

If in addition to studies of the steady-state characteristics of a discharge, such as running voltage or conductivity, one wishes to measure transient processes, such as diffusion, attachment, or recombination, one may use the methods to be discussed in this section.

If electrons or ions are present within a cavity resonant at microwave frequencies, they interact with the electric and magnetic fields inside the cavity. The magnetic interaction is negligible compared to the electric interaction. Furthermore, the positive ions have a negligible effect, for their interaction is about $10^{-3}$ that of the electrons with the electric field. As a result, one may observe the behavior of the electrons alone by means of a microwave field. It is possible, by methods discussed in the next section, to relate the electron density within the cavity to the resonant frequency of the cavity-and-electrons combination. Therefore, it is sufficient to measure the resonant frequency of the microwave cavity containing electrons in order to determine the density of electrons within the cavity. In transient processes, where electron density changes with time (by diffusion, attachment, or recombination), measurements of the resonant frequency of the cavity as a function of time can be used to determine diffusion coefficients, attachement probabilities, or recombination coefficients, depending on the dominant removal process of the gas being studied.

4.1. Resonant Frequency Shift of a Cavity as a Function of Electron Density within the Cavity. It has been shown that for small changes in conductivity, the resonant frequency shift of a cavity is given by:

$$\frac{\Delta\nu_o}{\nu_{oo}} = \frac{1}{2} \frac{\int_{vol.} \left(\frac{\sigma_1}{\omega\epsilon_o}\right) E_o^2 dV}{\int_{vol.} E_o^2 dV} \qquad (4\text{-}1)$$

where $\nu_{oo}$ is the resonant frequency of the cavity in the absence of electrons, $\Delta\nu_o = \nu_o - \nu_{oo}$ is the change in the resonant frequency due to the presence of the electrons, $E_o$ is the peak electric field at a point in the cavity, $\sigma_1$ is the imaginary conductivity due to the electrons within the cavity and $\epsilon_o$ is the permittivity of free space.

From kinetic theory it can be shown that the imaginary part of the complex conductivity is approximately related to the electron density by:

$$\sigma_i = \frac{ne^2}{m\omega} \tag{4-2}$$

where e and m are respectively electron charge and mass, $\omega$ is applied radian frequency, and n the electron density.

The usual experimental arrangement consists of a $TM_{010}$ cavity with a cylindrical quartz (or glass) container centered inside it as in Fig. 4-1. Considering the center of the cavity as origin, the simplest

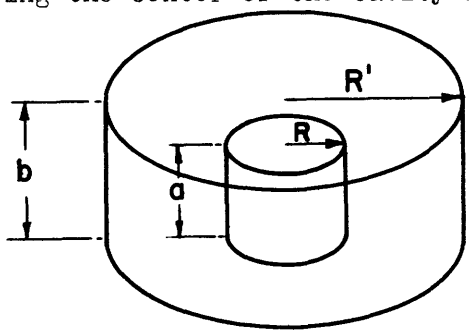


Fig. 4-1. Experimental cavity and gas bottle arrangement.

electron distribution within the bottle is

$$n = n_o \left\{ J_o\left(\frac{2.405}{R} r\right) \cos\left(\frac{\pi}{a} z\right) \right\} . \tag{4-3}$$

In transient processes $n_o$ and hence n varies with time, but the spatial form is unchanged. The amplitude of the field within the cavity is given by

$$E_o = E_m J_o\left(\frac{2.405}{R'} r\right) . \tag{4-4}$$

In the numerator of Eq. (4-1) we may replace the Bessel function variation of $E_o$ by the first two terms of its power series expansion provided R is appreciably smaller than R'. Thus

$$E_o \simeq E_m \left\{ 1 - \left(\frac{2.405}{2R'} r\right)^2 \right\} . \tag{4-5}$$

Equation (4-1) becomes:

$$\frac{\Delta\nu_o}{\nu_{oo}} = \left( \frac{n_o e^2}{2m\omega^2 \epsilon_o} \right) \left(\frac{2a}{\pi h}\right) \frac{\int_o^R \left\{ rJ_o(kr) - 2fr^3 J_o(kr) + f^2 r^5 J_o(kr) \right\} dr}{\int_o^{R'} rJ_o^2(\ell r) dr} \tag{4-6}$$

where

$$k = \frac{2.405}{R} ,$$

$$\ell = \frac{2.405}{R'} ,$$

and

$$f = \left(\frac{2.405}{2R'}\right)^2 = \frac{\ell^2}{4} .$$

Equation (4-6) may be evaluated by successive partial integrations and the result is

$$\frac{\Delta\nu_o}{\nu_{oo}} = \left(\frac{n_o e^2}{m\omega^2\epsilon_o}\right)\left(\frac{a}{\pi h}\right)\left[1.60\left\{\frac{R}{R'}\right\}^2 - 1.42\left\{\frac{R}{R'}\right\}^4 + 2.58\left\{\frac{R}{R'}\right\}^6\right]. \quad (4-7)$$

Thus for $\sigma_1/\omega\epsilon_o \ll 1$ we may estimate the electron density within the cavity by measurements of the resonant frequency shift of the cavity.

4.2. The Transmission Method. As noted in the previous section, one of the simplest resonant cavities suitable for our purposes is the cylindrical $TM_{010}$ cavity. Coupling into and out of the cavity is achieved by means of coupling loops. The gas sample is contained in a cylindrical quartz bottle which is placed within the metal cavity.

A simplified block diagram of the apparatus used in the transmission method is given in Fig. 4-2. The cavity containing the quartz bottle

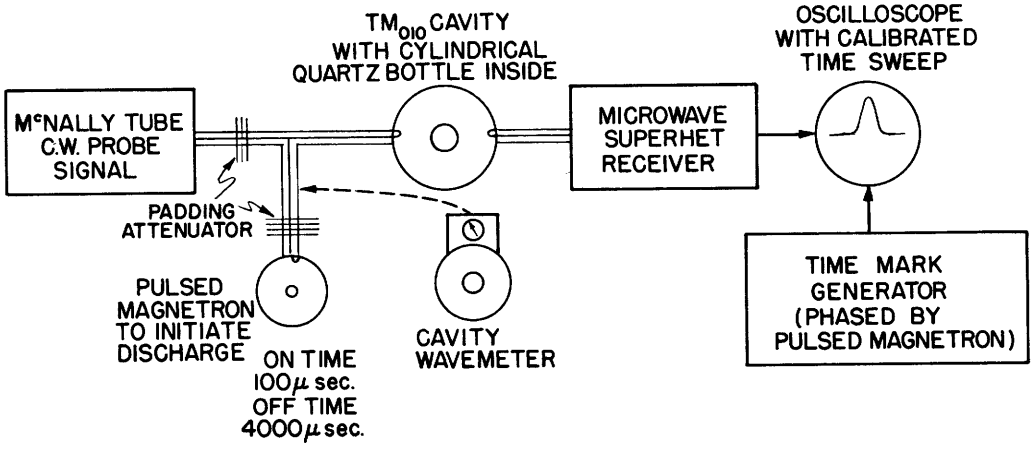


Fig. 4-2. Simplified block diagram of experimental apparatus for transmission method.

into which gas samples are introduced is at the center of the diagram. A discharge is initiated in the gas by means of a large r-f field from the pulsed magnetron at the left. A discharge lasting approximately 100 μsec is found to be necessary in order to have a steady-state distribution of the ions and electrons in the bottle. At the end of this period the magnetron is turned off for 4000 μsec. During this time the ions and the electrons diffuse to the walls of the cavity (for pure helium at pressures of the order of mms of mercury) and recombine there to form neutral atoms. The whole cycle is then repeated. Measurements are made during the 4000-μsec interval when the magnetron is off, and the ions and electrons are diffusing to the walls. A small c-w signal is fed into the cavity from the reflex klystron (Type 2K28) at the left. As the electron density in the cavity varies, the transmission of the signal through the cavity varies in the following manner: If we consider the cavity in the absence of free electrons, a c-w signal whose frequency is set to the resonant frequency of the "empty" cavity, $\nu_{oo}$, will undergo maximum transmission through the cavity. Signals of frequencies different from $\nu_{oo}$ will undergo reduced transmission.

In Sec. 4.1 we showed that the presence of electrons within the cavity acts to increase the resonant frequency of the cavity. Thus if the c-ω signal is set to a frequency higher than $\nu_{oo}$, it will undergo maximum transmission through the cavity when the residual density of electrons (i.e. those electrons which have not as yet diffused to the walls) and the cavity constants give a resultant resonant frequency equal to that of the c-w signal. Since the electron density varies with time, we will get a transmitted signal which is at first small when the cavity-and-electrons resonant frequency is larger than the frequency of the c-w signal. Then, as $\nu_o$ of the cavity-and-electrons approaches the signal frequency, the transmission increases, reaching a maximum approximately when $\nu_o = \nu_{sig}$ and then decreases as $\nu_o$ moves below the signal frequency.

A series of measurements of time of maximum transmission versus signal frequency are made. The data are related by Eq. (4-7) to the density of electrons in the gas as a function of time. One plots the resonant frequency shift $\Delta\nu_o$ versus time, and from the decay constant of the curve determines the desired gas coefficients (e.g. for helium, the ambipolar diffusion coefficient).

It should be pointed out that this method is suitable for determining the transient properties of electrons at thermal energy (0.03 ev). The origin of time in our measurements occurs at the instant when the magnetron is turned off. At this instant a highly ionized gas is present within the quartz bottle, and the electrons in the gas have a mean energy of the order

of several volts. The electrons quickly lose energy by elastic collisions, however, and reach thermal equilibrium with the gas in from 10 to 50 μsec. Since observations are made over a 4000-μsec period the first 50 μsec can be neglected.

4.3. The Reflection Method. Since actual equipment does not approximate the idealized circuit of Fig. 4-2, analysis of the transmission method from the microwave standpoint is rather involved. The padding attenuators, for example, are somewhat reactive and their susceptance varies erratically with frequency. This effect complicates the problem of relating maximum power transmission through the cavity to the resonant frequency of the cavity. The reflection method, on the other hand, lends itself to a simple and straightforward analysis although an additional variable is introduced into the experimental measurements. Consider a cavity and a length of transmission line coupled into the cavity by means of a coupling loop. At resonance the line appears to be terminated in a pure resistive load. A standing-wave pattern is set up with minima occuring every half wavelength down the line. Suppose a slab of dielectric is inserted in the cavity; then the resonant frequency would change and consequently the locations of the resonant minima of the standing-wave pattern.

If free electrons are present in the cavity, they act as a negative dielectric, altering the resonant frequency of the cavity in proportion to their concentration. In order to obtain data to measure this effect, it is necessary to know at which points in the line the resonant minima are located as a function of the resonant frequency of the cavity-and-electrons combination. We obtain this curve in the following way: The cavity is shorted by some means (e.g. a metal post is inserted at its center) and using a standing-wave detector and slotted section one measures the location in the line of a minimum as a function of the frequency of the signal incident upon the cavity. These data correspond to the condition of anti-resonance of the cavity. The location of the resonant minima are obtained from these data by adding or subtracting a distance equal to one quarter wavelength. A straight line is obtained as in Fig. 4-3. The use of this curve is described in the following paragraphs.

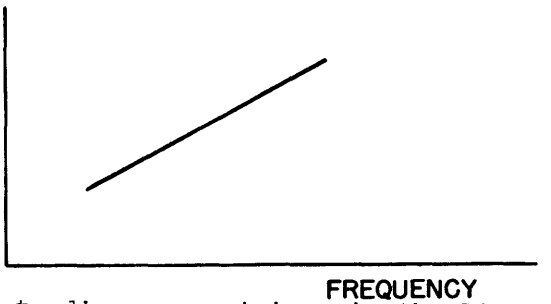


Fig. 4-3. Position of the standing-wave minimum in the line as a function of the resonant frequency of the cavity.

A block diagram of the apparatus used in the reflection method is shown in Fig. 4-4. The similarity to the transmission method shown

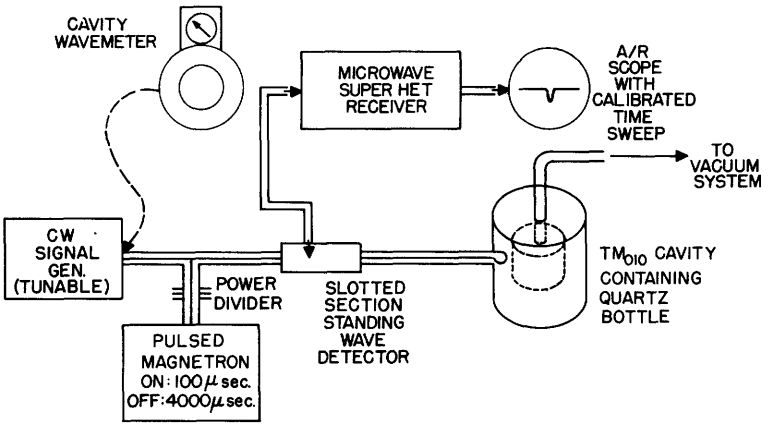


Fig. 4-4. Simplified block diagram of the experimental apparatus for the reflection method.

in Fig. 4-2 is at once apparent. The cavity is at the far right and now has only an input coupling loop. A slotted section has been added and the signal from its pickup probe is applied to the mixer of the microwave receiver. In other respects the equipment is unchanged.

As before, the gas in the quartz bottle is ionized by the r-f pulse from the magnetron, which is then turned off for 4000 μsec. The c-w signal is incident upon the cavity from the left. The standing-wave pattern set up in the line is picked up by means of the slotted-section probe.

Suppose the c-w signal is set to a frequency higher than the "empty" resonant frequency of the cavity and the standing-wave detector probe is set to the resonant minimum position corresponding to this frequency. Because of the change in electron density in the cavity, the resonant frequency changes. At first the resonant frequency is above the signal frequency, but as time passes the resonant frequency approaches the signal frequency and then passes below it. Simultaneously, the position of the minimum of the standing-wave pattern changes location because of the changing impedance of the cavity. When the cavity resonates with the signal frequency, the minimum of the standing-wave pattern is at the probe position. As the impedance changes off resonance, the minimum moves away from the probe. Thus at the time at which the cavity resonant frequency equals the c-w signal frequency, the minimum of the standing-wave pattern passes the pickup probe and a dip in the response on the scope is noted.

Experimental procedure is as follows: The c-w signal is set to a given frequency, and this frequency is measured by the cavity wavemeter. The standing-wave probe is set to the proper point in the line (from the curve given in Fig. 4-3) and the time of minimum response is noted. Then the signal frequency is changed to a new value and measured, the probe ad-

justed to the new location in the line, and the new time of minimum response is noted. From a series of these measurements $\Delta\nu_o$ as a function of time is determined and the desired gas coefficient is evaluated as before.

The simplicity of this method lies in the fact that the impedance of the various components to the left of the slotted section do not enter into the calculations. In addition, this experiment may be extended very easily to measure the Q of the cavity as a function of time. From this measurement, additional information about the gas under study may be obtained.

4.4. Transient Measurements of the Standing-Wave Pattern. Measurement of the transient behavior of a discharge after the exciting voltage is removed may be made by using circuits that measure a current or voltage during a selected short time interval. For this purpose the standing-wave pattern in a waveguide or other transmission system is a convenient parameter, as it may be related to the desired properties of the discharge. Consequently a method has been devised to permit measurement of standing-wave pattern during a short time interval, the time coordinate of this interval being adjustable over a considerable range. It is assumed that the properties of the discharge do not change appreciably during the time of measurement.

The method is shown schematically in Fig. 4-6. A gas discharge is formed in a cavity, section of transmission line, or other container arranged to permit examination of its dielectric properties. In the method illustrated a microwave oscillator delivers a weak signal to the discharge through a slotted section, which allows exploration of the standing-wave pattern set up by the discharge. A modified spectrum analyzer (TSS-4SE) is used as a detector of this standing-wave pattern, and its video output is displayed on the screen of the A/R scope.

Because the discharge is pulsed, the pattern is a function of time, and the spectrum analyzer must now be arranged to indicate voltage during a short time interval which can be adjusted to cover the range of time of interest. This is accomplished by use of the delay multivibrator circuits in the A/R scope, which are triggered by the same timing pulse that triggers the discharge. The length of the delay is determined by the delay control on the A/R scope. At the end of the delay period a sawtooth sweep voltage is applied to the horizontal plates of the cathode-ray tube in the A/R scope, an intensifier pulse is applied to the grid of the tube, and a small fraction of the sweep voltage is applied to the reflector electrode of the 707-B oscillator in the spectrum analyzer. The average reflector voltage and the sweep voltage are adjusted in such a way that the local oscillator reaches the frequency necessary to pass a signal through the spectrum analyzer while the reflector electrode is being swept (and thus

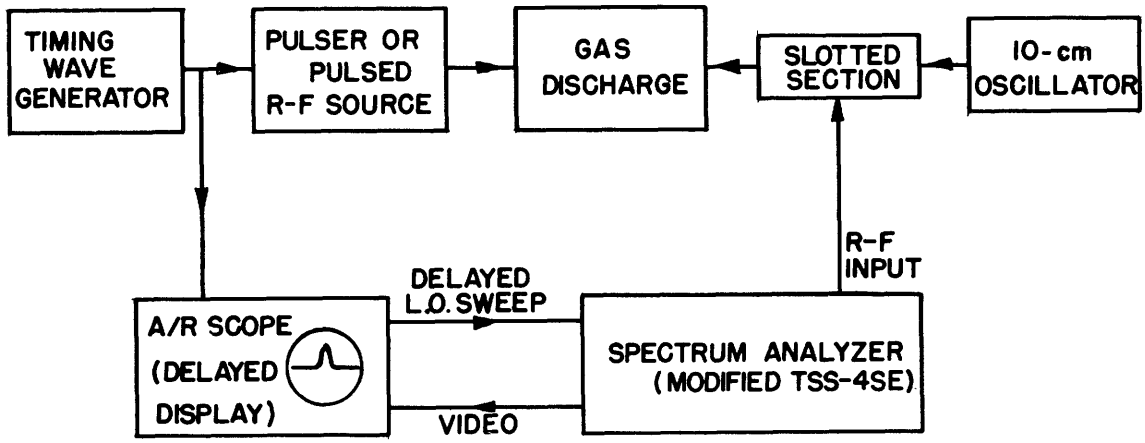


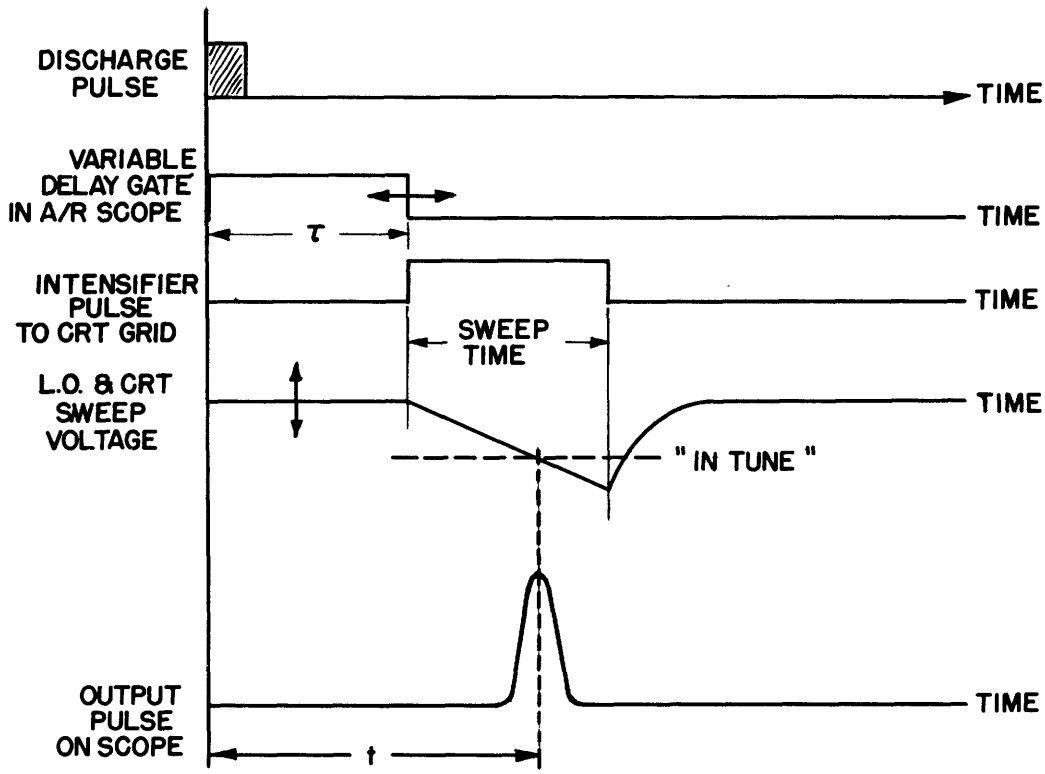


Fig. 4-5. Simplified schematic and time diagrams for transient measurement of standing-wave pattern.

while the cathode-ray tube receives an intensifier pulse and horizontal sweep voltage).

Because the local oscillator frequency sweeps past the frequency necessary to send a signal through the i-f amplifier, the output of the spectrum analyzer appears as a pulse on the A/R scope screen. Sweep lengths of approximately 5, 12, and 24 μsec are available, and these may be obtained with delays up to nearly 1200 μsec. Because these sweeps are so rapid, a bandwidth problem now occurs, for the normal half-power bandwidth in the spectrum analyzer of about 75 kc/sec cannot transmit a pulse created by sweeping through this bandwidth in 24 μsec without considerable attenuation and broadening of the pulse. An i-f amplifier with a bandwidth of 184 kc/sec has been found acceptable with the 24-μsec sweep, and one of 3 Mc/sec is more than ample for the 5-μsec sweep.

The relations between bandwidth, sweep speed, and transmitted pulse characteristics may be summarized in the following approximate relations. Let F be the total frequency range over which the local oscillator frequency is changed linearly during a time interval T, and let the bandwidth be B. Then the smallest transmitted pulse width obtainable with a given rate of frequency sweep, F/T, occurs when

$$F/T = 2B^2 .$$

If the ratio of the half-power width of the transmitted pulse to the total frequency sweep F is W, then

$$FT = (k/W)^2,$$

where k is found experimentally to be approximately 1.3.* From these equations one obtains directly

$$T = \frac{1}{\sqrt{2}\,B}\left(\frac{k}{W}\right),$$

$$F = \sqrt{2}\,B\left(\frac{k}{W}\right).$$

Thus the frequency interval and sweep duration for minimum pulse width are determined separately from W, the fraction of the sweep length occupied by

*For a further discussion of these equations see: E. N. Williams, "Radio-Frequency Spectrum Analyzers", Proc. I.R.E., 34, 18P (1946); and G. H. Sloan, Master's Thesis, Department of Physics, M.I.T., 1947.

the transmitted pulse, and from the bandwidth. If W is less than about 1/4, the pulse occupies too large a fraction of the sweep to permit easy measurement; whereas if it is very much larger, the required accuracy of measurement of time on the sweep increases, and no compensating advantages appear. A good working range for k/W appears to be from about 6 to 10.

Circuit Diagram. The details of the circuit modifications are shown in Fig. 4-6. In addition to the wiring changes shown it was necessary to take special precautions to eliminate very small 60-cycle modulation of the frequency of the oscillator. Special shielding of some leads was required, and as a final step it was found necessary to use a repetition frequency of 60 cps, synchronized with the power line voltage. The video amplifier is a single 6AC7 with a 15K plate load resistor.

Method of Operation. The time at which standing-wave ratio is to be measured is chosen, and the delay time $\tau$ is set by the range dial on the A/R scope to slightly less than this value (see Fig. 4-5). The d-c reflector voltage is then varied until the sawtooth sweep voltage passes through the value that results in the correct intermediate frequency (this value is indicated by the horizontal dotted line). The total delay time t is then the time $\tau$ plus the time from initiation of the sweep to the maximum of the pulse. The standing-wave ratio or other customary transmission

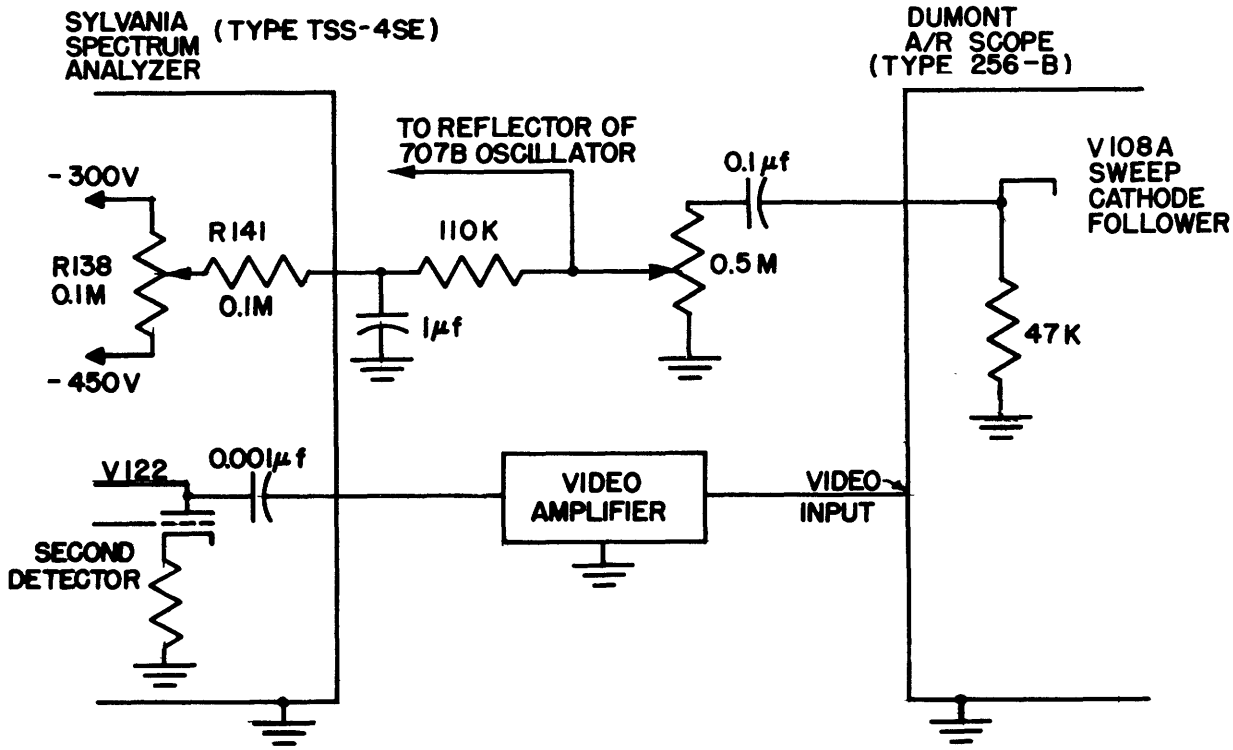


Fig. 4-6. Circuit diagram showing modifications of spectrum analyzer and A/R scope for fast sweep.

line measurements are made for this setting of time delay; then the delay may be readjusted and the measurements repeated. As an example, measurements may be quoted which were obtained with the coaxial-line discharge device shown in Fig. 4-7. (See the July 15, 1947, RLE Quarterly Progress Report, p. 22 for further details.) The fine center wire is pulsed for 1 μsec by a radar modu-

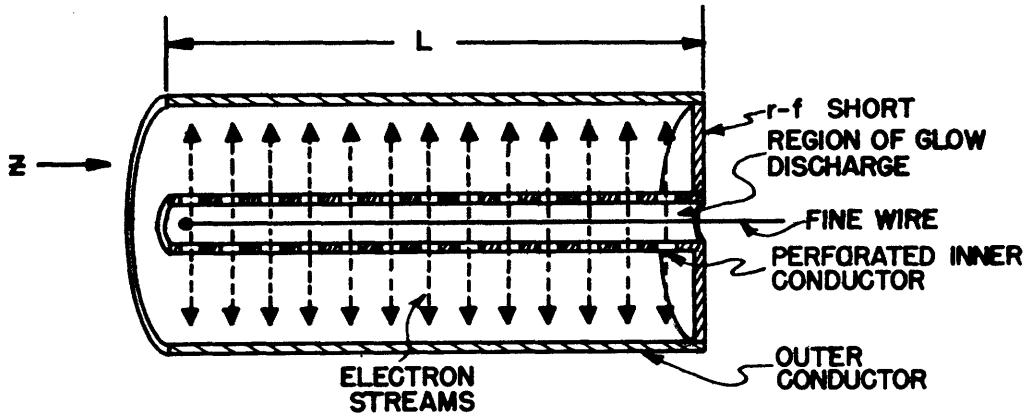


Fig. 4-7. Coaxial discharge construction.

lator. The standing-wave ratio at a wavelength of 10 cm varies about 35 db at a time delay of 8 μsec, to 49 db at about 100 μsec and beyond. The shift in the minimum position at 8 μsec is about 2 mm. Thus the dielectric properties of the discharge can be determined from a time shortly after the discharge is terminated to the time when its effects have become unmeasurable.

Limitations of the Method. The assumption underlying the sweep method is that the phenomenon to be observed does not change its characteristics appreciably during the sweep time T. If extremely fast discharge decay is to be observed T will be required to become so small that more elaborate circuit arrangements will be necessary.

It is further assumed that the properties of the discharge repeat after each pulse. (In the example given above, there is sufficient lack of uniformity from pulse to pulse that precise measurements are not possible.)

A minor inconvenience of the arrangement shown in Fig.4-5 is that the average reflector voltage cannot be set to place the pulse near the front or middle of the sweep, because in this range sufficient signal passes through the amplifier on the side of the resonance curve to paralyze the i-f amplifier, and when the correct local oscillator voltage is reached the gain is low. This difficulty is avoided if the pulse is set well toward the end of the sweep. It could be corrected by increasing T or by starting the local oscillator sweep a sufficient length of time before the cathode-ray tube sweep, and by readjusting the two sweep lengths accordingly. This step, however, has not yet been considered necessary.